THE CALIBRATION, VALIDATION, AND COMPARISON
OF VISSIM SIMULATIONS USING THE TWO-FLUID MODEL

by

JEREMY McCANDLESS CROWE
B.S. Florida Institute of Technology, 2007

A thesis submitted in partial fulfillment of the requirements
for the degree of Master of Science
in the Department of Civil and Environmental Engineering
in the College of Engineering and Computer Science
at the University of Central Florida
Orlando, Florida

Summer Term
2009

UMI Number: 1472159

ABSTRACT

The microscopic traffic simulation program VISSIM is a powerful tool that has been used by transportation engineers and urban planners around the world. A VISSIM simulation is meant to depict the performance of the physical road network through the use of modeling tools and behavioral parameters. The process which gets the model to the point of matching real world conditions is called calibration and requires a means of relating the real world to the simulated world. The topic of this thesis discusses a new means of calibration using the two-fluid model. The two-fluid model is a macroscopic modeling technique which provides quantitative characteristics of the performance of traffic flow on an urban road network. The model does this by generating a relationship between the travel time, stopped time, and running time per mile. The two-fluid model has been used to evaluate the performance of road networks for decades but now it is possible to use it to calibrate a VISSIM model. For this thesis, the two-fluid model to be used for calibration was generated from data collected on the Orlando, Florida, downtown network in February, 2008, during three traffic peaks for three typical weekdays. The network was then modeled in VISSIM which required a large amount of data regarding network geometry, signal timings, signal coordination schemes, and turning movement volumes. A similar data collection exercise was conducted during November, 2008, to capture the effects of changes that took place in the network during the ten month period. Another VISSIM network was also made to match the conditions of the November network. The February field data was used to successfully calibrate the VISSIM model and the November data was used to validate the calibrated network. The validation proved that the two-fluid models from the November field data and VISSIM data are statistically similar. With the network calibrated and validated, it could be used to perform scenario tests to see how the network performance would be affected

by changes to the network. The two-fluid model has often been used to compare two different physical networks or explore how the performance of a single physical network has changed over time. A similar comparison can be done with the two-fluid models from a calibrated, simulated network. By using the original calibrated models as base cases, scenarios ranging from lane closures due to traffic incidents to the addition of a whole new signalized corridor on the network can be modeled in VISSIM and compared with the corresponding base case. This would allow a governing agency to preview the effects of proposed changes.

ACKNOWLEDGMENTS

First, I would like to thank Dr. Radwan, the head of my committee and my advisor, for all the support and direction he has provided over the life of this project, thesis, and my graduate education. He has provided the perfect balance of motivation to finish and freedom to get the job done right. A huge thanks to Dr. Vinayak Dixit, also a committee member, is deserved for his incredible research assistance and instruction even when I didn’t understand things the first time. Even after leaving the University of Central Florida he has continued to teach me. I would also like to thank the final committee member, Dr. Mohamed Abdel-Aty, for being willing to step up and be a part of the work that has been accomplished. Also, special thanks goes out to Charles Ramdatt, Chris Kibler, John Rhodes, Albert Perez, and everyone else at the City of Orlando Transportation Dept. for their openness and provision of data and clarification, without which this project would not have been possible. Many thanks are also due to Premchand, Chris, Noor, Rami, and Mutasem for getting in the trenches and helping out with the thrill of field data collection. I am also thankful for friends like Taylor and Ali and especially for my family for the moral support they have provided through everything. The little things really do count.

TABLE OF CONTENTS

LIST OF FIGURES

LIST OF TABLES

CHAPTER 1: INTRODUCTION

For many decades, the two-fluid model has been used as an accurate way to measure the performance of surface street networks. The two-fluid model describes the relationship between the travel time and stopped time. The parameters of the model are representative of network performance. One way the two-fluid model has been used is to compare the same network at two different times. For example, say a two-fluid model is developed for a city using data collected from the present network. Then, several network changes are performed over the next few years such as road extensions, one-way to two-way conversions, and traffic signal offset corrections. After construction is complete, data for the two-fluid model is collected again and a new model is developed. These two models from different years on the same network can be compared to see how the network improvements affected performance.

All the work described above has been restricted to the physical world where the two-fluid model is used for post implementation evaluation in that it is only useful after the changes have been made. However, if it was possible to generate the new two-fluid model before the changes are made, the city could use such knowledge when deciding if the proposed network changes will have the desired result. Such a concept, which is the purpose of this thesis, is made possible by building the current network in the microscopic simulation software VISSIM 4.3 and then calibrating it to the two-fluid model formed using data collected from the actual network. This calibrated network model can then be modified to match the proposed changes. Using the data collection tools in the VISSIM software and a Matlab program to sort through the data, the two-fluid model can be constructed for the simulated network. This model can be compared to the model generated from data collected on the current network to evaluate if the proposed changes will improve performance.

There are three primary components of the research described in the following thesis: the formulation of the two-fluid model from field data; the construction, calibration, and validation of the VISSIM network; and the testing and comparison of different network scenarios. All of these research tasks were performed using the Orlando, Florida, downtown network as the project area. The two-fluid model chapter gives a basic introduction to how the two-fluid model is created using travel time and stopped time data. Collection of this data occurred on the Orlando downtown network in February and November of 2008. The February data was used for the VISSIM model calibration and the November data was used for validation. The data collection procedure used in both of these months is presented along with the analysis of the data which ultimately produced the two-fluid models.

A large step in the process of this thesis was the construction of a simulated network in VISSIM that reflected as closely as possible the conditions experienced during data collection. Network construction involved a combination of geometric data, signal timing information, and volume and turning movement data. A network matching the February data collection was created first and then a similar network matching the November data collection conditions was constructed.

In the VISSIM model calibration chapter, data is collected from VISSIM simulations using a procedure developed for this project. VISSIM data collection involved running the simulation and using the collected vehicle record data to distill travel time and stopped time data to ultimately develop a two-fluid model for the simulated network. In order to manipulate the simulation's performance, two different driving behavior parameters affecting driver aggressiveness were modified, within reason. An iterative process was applied until the VISSIM generated two-fluid model was as statistically similar as practical to the February field data two-fluid model. The validation of the network followed the same procedure as the calibration except no iterative process was required since the November two-fluid model simply had to be compared to the VISSIM simulation two-fluid model.

The final chapter deals with the description and comparison of different scenarios within VISSIM. First, a base case for the AM and PM traffic peaks was established for the Orlando downtown network using the November 2008 VISSIM networks. Additionally, two more base cases, which represented what the AM and PM networks could be like in the year 2015, were also created using data provided by the City of Orlando. With the four base case networks established, seven more scenarios were created and compared with the base case they were derived from. Once again the City of Orlando provided different contingencies they wanted to see the effects of. The results of these comparisons and how to interpret them will be discussed in detail.

CHAPTER 2: LITERATURE REVIEW

2.1: The Two-fluid Model

The two-fluid theory was developed by Prirgogine and Herman [1] to characterize traffic flow on an urban network. The two-fluid model assumes that vehicular traffic in an urban network can be differentiated as stopped vehicles and running vehicles. These models were constructed between the average travel time per mile (T) versus the average running time per mile (T_r) using regression as shown in Equation 1. The parameters (n, T_m) determined from the regression model are indicative of the quality of service of the networks. This also translates to the relationship between stopped time per mile and travel time per mile shown in Equation 2.

$$T_r = T_m^{\frac{1}{n+1}} T^{\frac{n}{n+1}} \tag{1}$$

$$T_S = T - T_m^{\frac{1}{n+1}} T^{\frac{n}{n+1}} \tag{2}$$

Mahmassani et al. [2] and Williams et al. [3] using computer simulation based on car following theory replicated the two fluid models on simple grid networks. It is interesting to note that T_m translates to the free flow travel time per mile and n determines how rapidly the travel time will increase as the stop time increases. Therefore, larger values of both T_m and n indicate worse network performance.

A quick and simple way of calculating T_m and n by restating Equation 1 as follows:

$$\ln T_r = \frac{1}{n+1} \ln T_m + \frac{n}{n+1} \ln T \tag{3}$$

Or, $\ln T_r = A + B \ln T$ (4)

where: $n = \frac{B}{1-B}$ (5)

$$T_m = e^{\frac{A}{1-B}} \quad (6)$$

All that is needed at this point is a means of finding A and B. Once the data for T and T_r are collected, $\ln T$ is plotted vs. $\ln T_r$. The regression line of this plot is in the form

$$y = Bx + A \quad (7)$$

Aredkani [4] in his Ph.D. dissertation showed that it was possible to model traffic flow on urban networks as a two-fluid model. The study was used to validate the ergodic assumption of the chase car methodology using aerial photographs. The ergodic assumption states that the ratio of stopped time per mile to the travel time per mile is equal to the ratio of the number of vehicles stopped to the total number of vehicles. This ergodic assumption is the core of the two-fluid model. Later, the author characterized and compared the two-fluid model for various cities as shown in Figure 1. Using the two-fluid model he concluded that Matamoros was the worst performing network and Austin was one of the better performing networks. The reason behind this conclusion is that the steeper the slope the more sensitive the travel time is to the stopped time, indicating that the network deteriorates more rapidly during congestion. It is also observed that the Matamoros two-fluid model has a higher intercept on the y-axis as compared to the model for Austin suggesting that even in un-congested conditions, drivers on the Matamoros network experience higher travel times compared to Austin drivers.

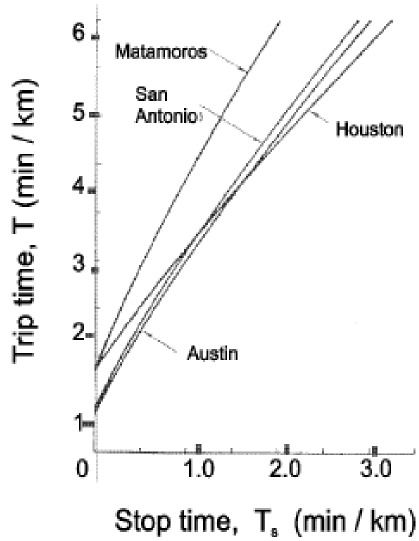

Figure 1: Two-Fluid model for various cities (Aredkani [4])

Recently Mattingly et al. [5] in a before-after study of networks observed that there had been no significant change in the performance of the network despite large number of projects to improve the network. On the contrary there had been a slight deterioration in the network shown in Figure 2.

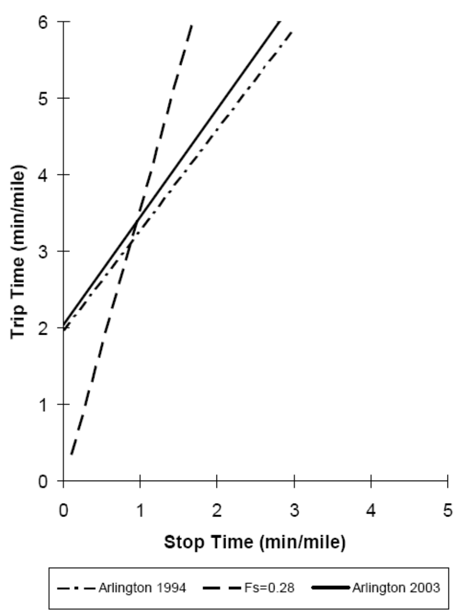

Figure 2: Comparison of Arlington (1994 vs. 2003) (Mattingly et al. [5])

In lieu of this, it is crucial to recalculate the two-fluid model regularly to monitor the performance of the network.

Ayadh [6], Ardekani et al. [7] and Bhat [8] selected various network features and estimated regression models to understand the effects of these network features on T_m and n. Table 1 summarizes the effects these network features have on the two parameters of the two-fluid model. The '+' and '-' signs indicate positive and negative effects respectively on T_m and n, as the associated factor increases. For example, an increase in signal density would increase T_m (depicted with a '+' sign) and decrease n (depicted with a '-' sign). In other words, an increase in the signal density would result in worse network performance during free flow conditions and better performance during congested conditions. These effects help provide general guidelines on how to interpret a two-fluid model comparison and on aspects that should be focused on to improve the operations of the network.

Table 1: Effect of various network features on the two-fluid model

Factors	T_m	n
Signal Density	+	−
Average Speed Limit	−	
Fraction of approaches with signal progression	−	
Average Number of Lanes per Street		−
Fraction of one way streets		+
Fraction with Actuated Signals		−
Average Block Lengths		+
Average Speed Limit	−	
Average Cycle Length	−	+

2.2: Established Calibration Methods

Even though the two-fluid model has been well established in the physical realm, its usage as a means of calibration and validation of a VISSIM microsimulation model is still untested. Before the two-fluid model can be evaluated as a calibration method, an understanding of established calibration guidelines, parameters, and methods for microsimulations is necessary. According to Dowling et al. [9], calibration of a model involves "the adjustment of model parameters to improve the model's ability to reproduce local driver behavior and traffic performance characteristics". One of the initial steps of the analyst is to determine those model parameters to adjust and those to keep fixed. If so desired, the model parameters to be adjusted can be subdivided into groups that will affect the simulation globally and those will affect it locally. The approach for calibration presented by Dowling et al. [9] recommends three steps: capacity calibration, route choice calibration, and system performance calibration. The results of these steps are bound by calibration criteria which establish acceptable levels of error between the field and the simulation. The acceptable error as cited by Dowling et al. [9] for various calibration criteria is <15% which translates to a >85% similarity between the results from the field and the simulation. There are also qualitative calibration criteria which include visual confirmation that elements such as bottlenecks and queuing on the network reflect actual conditions to the analyst's satisfaction.

Jha et al. [10] presents the development and calibration of a large scale microsimulation model. Four elements were modified for calibration: the parameters of the driving behavior model, parameters of the route choice model, the origin-destination (O-D) flows, and habitual travel times. Even though it was desired to calibrate all four elements simultaneously, the network size and computational time involved led the driving behavior to be calibrated first, separately, followed by the other three elements. These three elements were all part of the process of estimating and calibrating the O-D matrix for the simulation. For microsimulations, O-D matrices and dynamic route assignment are usually preferred due to their ability to route traffic in a realistic manner automatically. This also requires a large amount of information and effort during the calibration of the model. In Toledo et al. [11] an O-D matrix was used as part of an approach for calibrating microscopic simulations with aggregate data. It was stated that O-D estimation involves three input sets: traffic measurements, a seed O-D matrix, and an assignment matrix. To provide the basis for an O-D matrix, Jha et al. [10] used the project area's Traffic Analysis Zones (TAZs) to supply the needed route and volume information. This was possible because the large project area allowed the TAZs to provide detailed enough information. However, for a medium or small project area, using the TAZ data might not be feasible for acquiring O-D estimates because of the loss of detail as a result of having fewer zones in the network.

If the two-fluid model is to be utilized as a calibration tool for microsimulations, it must be able to accomplish the same goals as established calibration methods. The question is, "What simulation parameters should be adjusted to calibrate the simulation to the two-fluid model?" Recall that Jha et al. [10] first performed a calibration of the driving behavior before moving on to the O-D estimation. According to a study in Herman et al. [12], the parameters of the two-fluid model are influenced by driving behavior. The study looked at the effects of two driving behavior extremes on the two-fluid model. One test car was instructed to drive aggressively and another instructed to drive conservatively with both vehicles on the same network at the same time. The resulting two-fluid models were found to be significantly different with T_m decreasing and n increasing as the driver behavior became more aggressive. Therefore, the two-fluid model generated by VISSIM can be modified by adjusting the driving behavior parameters to make drivers more aggressive or more conservative. As for the O-D estimation, recall that the two-fluid model is a macroscopic evaluation tool and so while correct network volumes are still needed, a fully calibrated O-D matrix may not be required.

CHAPTER 3: DATA COLLECTION

In order to properly calibrate the simulated network using the two-fluid model, data collection was performed on the physical network to determine the two-fluid models to be used as a basis for each traffic peak. Figure 3 shows the area of downtown Orlando considered in the data collection. To ensure that the models reflected the average operating conditions, standard weekdays not designated as holidays were selected. For the purposes of this project, only two rounds of data collection were necessary. The first occurred in February of 2008 during a time when several links on the network were closed or narrowed due to construction activities at the SR-408 and I-4 interchange. The model generated from this round was used for the simulation calibration. The second round of data collection occurred in November of 2008 after most of the construction affecting the surface street network had been completed. The model generated from this data was used to validate the simulation's calibration and to provide the City of Orlando with a base case to compare future two-fluid models.

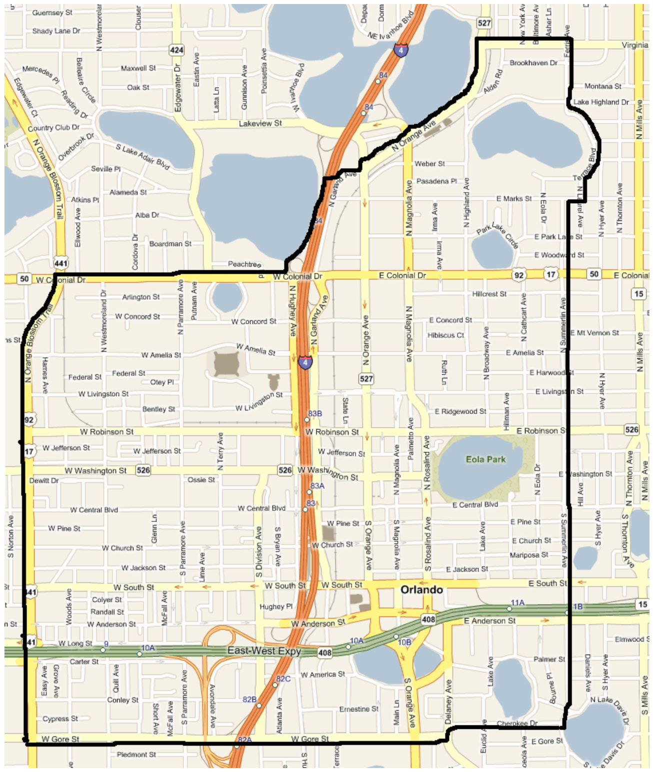

Figure 3: Orlando Downtown Network Project Area
(http://local.live.com/, April 20, 2007)

3.1: Methodology

Data was collected using the “chase car” methodology for the AM, Midday and PM peaks. In the chase car methodology, the chase car follows a random vehicle until it leaves the project area, parks, or performs a maneuver the chase car driver cannot match safely or legally. After losing a vehicle, the chase car is driven normally with respect to adjacent traffic until the next convenient vehicle to be followed is selected. By using the chase car method, it is expected that the study area is sampled according to the behavior of drivers traveling through and in the network.

For the purposes of the two-fluid model, travel times and stopped times are the only essential information to be collected. For this project, two techniques were used to collect this necessary data. The first technique, called the one-mile method, used the chase car’s trip odometer to determine when a mile had been traveled and involved using two stop watches to measure the travel time and stopped time during that mile. The second technique, called the two-minute method, involved using one stop watch to time up to two minutes while the other stopwatch was used to measure stopped time. Also, the trip odometer readings are recorded for the beginning and the end of the two minutes. Both data collection techniques required the same material and personnel per chase car: a driver, a data collector, and two stop watches. The tasks of the data collector included recording the odometer readings, the absolute times from the stopwatch and the number of stops for the duration of each trip.

The two data collection methods are fundamentally different in how they gathered travel and stopped time data. The one-mile method measures this driving behavior over distance while the two-minute method measures it over time. Since only one method was desired for use in the calibration and validation, a decision had to be made as to which one to use to generate the two-fluid models from the physical and simulated network. Several advantages and disadvantages exist for each of the two data collection methods. It should be noted that, according to Mahmassani [2], travel time and stopped time over a fixed distance are two of the three principal variables of which the two-fluid model is a relationship (the third being running time). Data collected using the one-mile method is in the form of travel time and stopped time which indicated a good connection between the one-mile method and the underlying theory. However, one disadvantage is that if travel times are being collected on a congested network, fewer data points will be collected because travel times per mile will be much longer than on a free flowing network. One way to remediate this would be to measure the travel times for trips that are a predetermined fraction of a mile and then calculate the travel time per mile later. This would also avoid the potential rounding errors of the two-minute method. Unfortunately, this remediation was not employed during data collection for this project.

For the two-minute method, the advantage is that no matter what the level of congestion on the network, it is guaranteed that a certain number of data points will be collected since the travel time per trip is fixed to two minutes. At the end of a two minutes trip, a new trip begins. However, a problem arises when, due to congestion, the chase car travels less distance than the trip odometer's ability to measure resulting in the potential for random errors when calculating the travel time. For example, say for a two minute trip, the chase car travels only 0.05 miles but the distance recorded is 0.1 miles. The actual travel time is 40 minutes but due to the rounding of the odometer, the calculated travel time is only 20 minutes, in other words, a percent error of 100%. This problem could be solved by measuring distance with a more accurate instrument which would reduce the percent error encountered for shorter trips. This, however, was also not employed during the data collection for this project.

Along with considering the advantages and disadvantages, the selected method also had to be easily imitated within VISSIM 4.3. This was ultimately the deciding factor since, as will be discussed in Chapter 5, it was deemed easier to collect data from VISSIM in the two-minute format instead of the one-mile format. However, this decision was made after data collection took place so the data collected was a mixture of both methods.

3.2: February 2008

For the February data collection round, the three typical weekdays selected were 2/19/08 (Tuesday), 2/20/08 (Wednesday), and 2/21/08 (Thursday). For each of these days, data was collected during the AM, Midday, and PM peaks which spanned from 7:30-9:00am, 11:45am-1:15pm, and 5:00-6:30pm, respectively. Two teams of data collectors were deployed for each day. Both teams used the one-mile method on Tuesday and the two-minute method on Wednesday. However, each team took a different method on Thursday. The reason the data collection methods were mixed over the three days is that, at the time, no preference was given to one method over another. For the one-mile method, data collected over the entire network was travel time, stopped time, and number of stops for each trip. For the two-minute method, the data collected was the starting and ending trip odometer reading, the stopped time, and the number of stops during the two minutes.

3.2.1: Data Analysis and the Two-Fluid Model

With the field data collected, it was entered into a spreadsheet and divided based on whether the one-mile or two-minute method was used, and then sub-divided based on the traffic peak. Appendix A shows how the raw data from February 2008 was organized. For the purpose of data analysis, each one mile or two minute trip counted as one point of data. As stated previously, even though both collection methods were employed, only the two-minute travel time data was used to calibrate and validate the VISSIM model. The raw data was used to calculate the travel time, running time, and stopped time, all in min/mile. The natural logs of travel time ($\ln TT$) and running time ($\ln RT$) were also calculated and placed in separate columns. Figure 4 shows a plot of $\ln RT$ vs. $\ln TT$ and the linear regression equations for each peak. Equation 7 was then applied to the regression equations from Figure 4 to obtain the values for terms A and B. These values were then plugged into Equations 5 and 6 to calculate the two-fluid model parameters T_m and n for the data from each traffic peak. Table 2 shows the regression terms used to generate the two-fluid parameters and the parameters themselves.

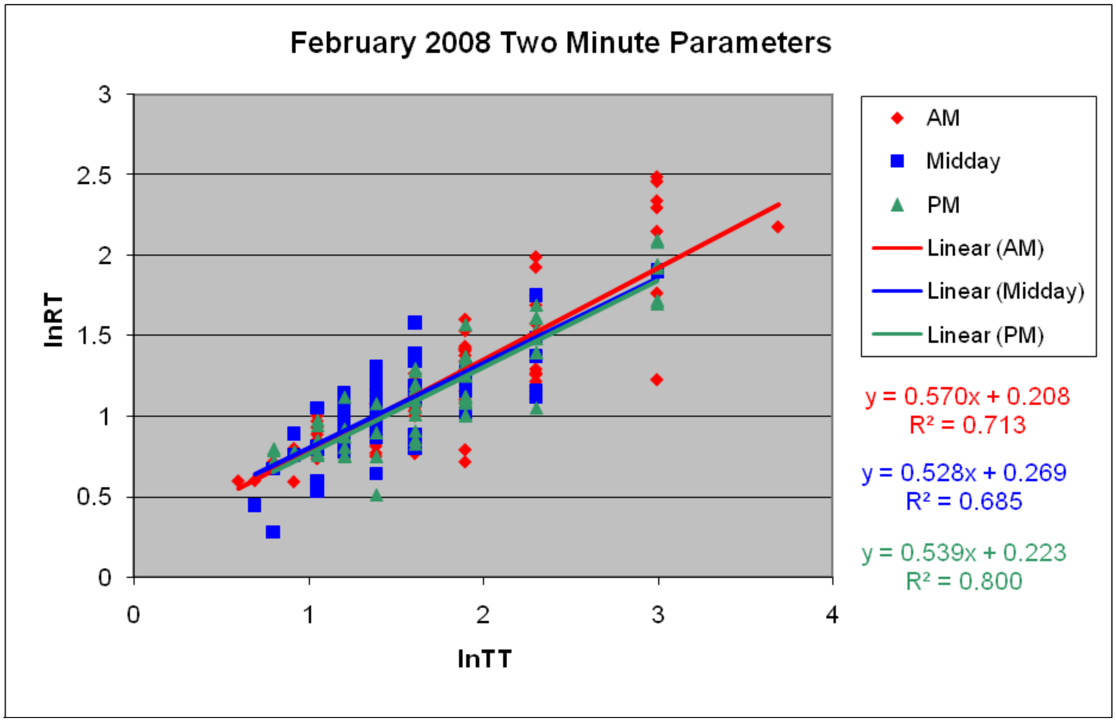

Figure 4: Regression Curves to Calculate Two-Fluid Model Parameters

Table 2: February 2008 Regression Terms and Two-Fluid Model Parameters

	Regression Term		Two-fluid Parameters	
Traffic Peak	A	B	T_m	n
AM	0.207995	0.570484	1.62	1.33
Midday	0.269913	0.528721	1.77	1.12
PM	0.223358	0.539130	1.62	1.17

With the two-fluid model parameters known, it was possible to generate a graphical representation of the two-fluid model. By plugging the parameters into Equations 1 and 2 and then assuming values for travel time (*T*) in 0.2 minute increments, a graph was made of travel time vs. stopped time showing the two-fluid model for each traffic peak. Figure 5 shows the AM, midday, and PM peak models generated using the procedure just described.

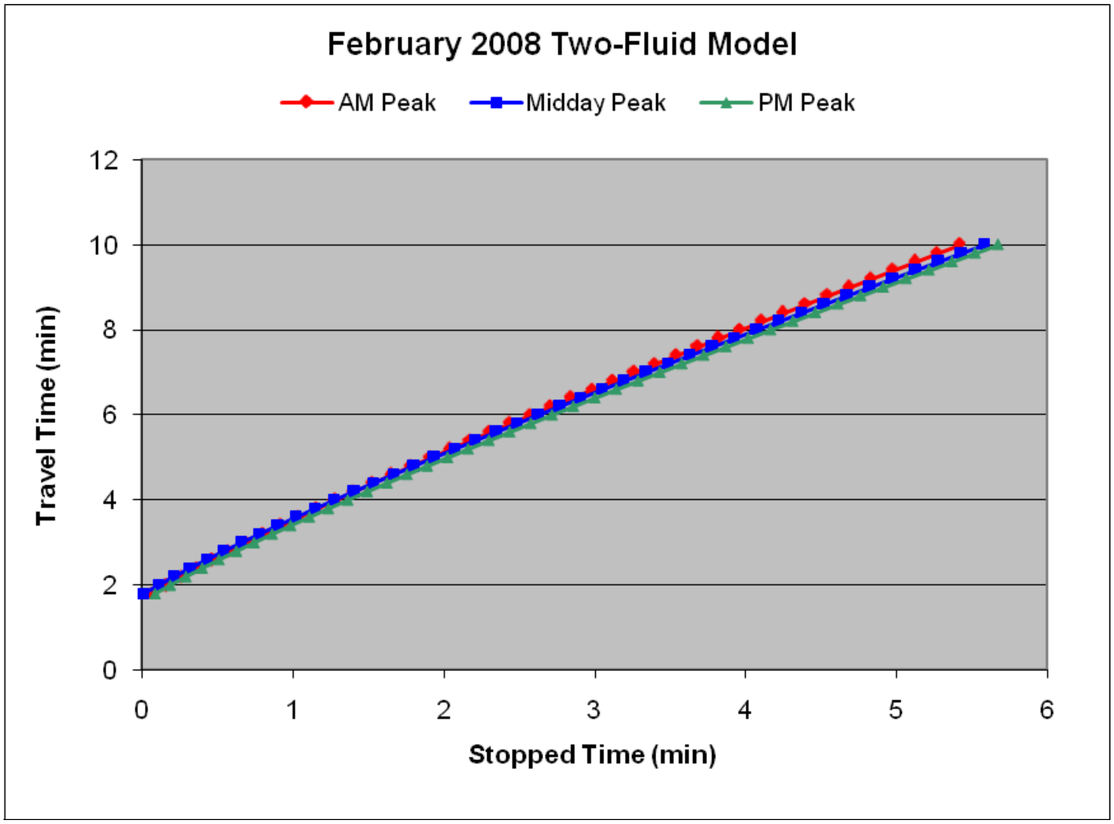

Figure 5: February 2008 Two-Fluid Models

The graphical representation can be used to perform a visual comparison of the two-fluid models from different networks or from different times on the same network as in Figures 1 and 2, respectively. A visual interpretation of Figure 5 reveals that all traffic peaks perfomed similarly in free flow conditions but as the networks became more congested, the PM peak maintained a lower trip time per mile for a given stopped time. The midday peak had slightly worse performance but the AM peak had the worst under congestion. These results can also be reached by reviewing the two-fluid parameters. Recall that the lower the values of T_m and n, or the shallower the slope, the better the network performance is. This method of comparison will be used throughout this thesis.

3.3: November 2008

For the November data collection period, the three typical weekdays selected were 11/10/08 (Monday), 11/12/08 (Wednesday), and 11/13/08 (Thursday). The reason Monday was selected instead of Tuesday was that Tuesday was designated as Veterans Day, an official holiday. As such, traffic on that day was expected to be less, creating atypical conditions for data collection. For each of these days, data was collected during the AM, midday, and PM peaks which spanned from 7:30-9:00am, 11:45am-1:15pm, and 5:00-6:30pm, respectively. As in February, two teams of data collectors were deployed for each day. Both used the one-mile method on Monday, the two-minute method on Wednesday, and went back to the one-mile method on Thursday. The reason for this change was that the one-mile method produces fewer data points per session than the two-minute method. Therefore, in order to produce about the same number of data points for each method, the one-mile method was used for two of the days. Just as in February, data collected over the entire network for the one-mile method was travel time, stopped time, and number of stops for each trip. For the two-minute method, the data collected was the starting and ending trip odometer reading, the stopped time, and the number of stops for each trip.

3.3.1: Data Analysis and the Two-Fluid Model

The same data analysis procedure used for the February data was applied to the November data. Appendix B contains the raw data after division by collection method and traffic peak. This raw data was converted to minutes per mile and used to calculate ln*TT* and ln*RT*. Figure 6 shows a plot of ln*RT* vs. ln*TT* and the linear regression equations for each peak. As with the February data, the terms in the regression equations were plugged into Equations 5 and 6 to calculate the two-fluid model parameters. Table 3 shows the regression equation terms and calculated two-fluid parameters. The graphical representation of the two-fluid model for the AM, midday, and PM peaks is shown in Figure 7.

Table 3: November 2008 Regression Terms and Two-Fluid Model Parameters

	Regression Term		Two-fluid Parameters	
Traffic Peak	A	B	T_m	n
AM	0.343170	0.440450	1.85	0.79
Midday	0.335750	0.541284	2.07	1.18
PM	0.517996	0.377754	2.26	0.63

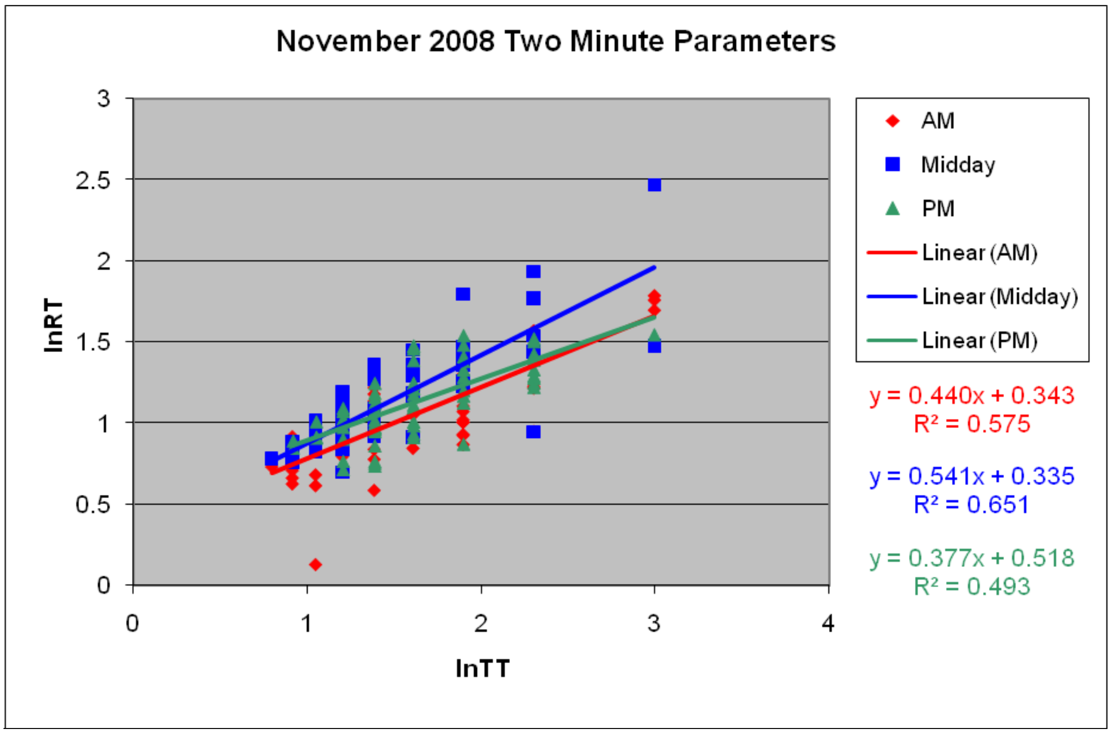

Figure 6: Regression Curves to Calculate Two-Fluid Model Parameters

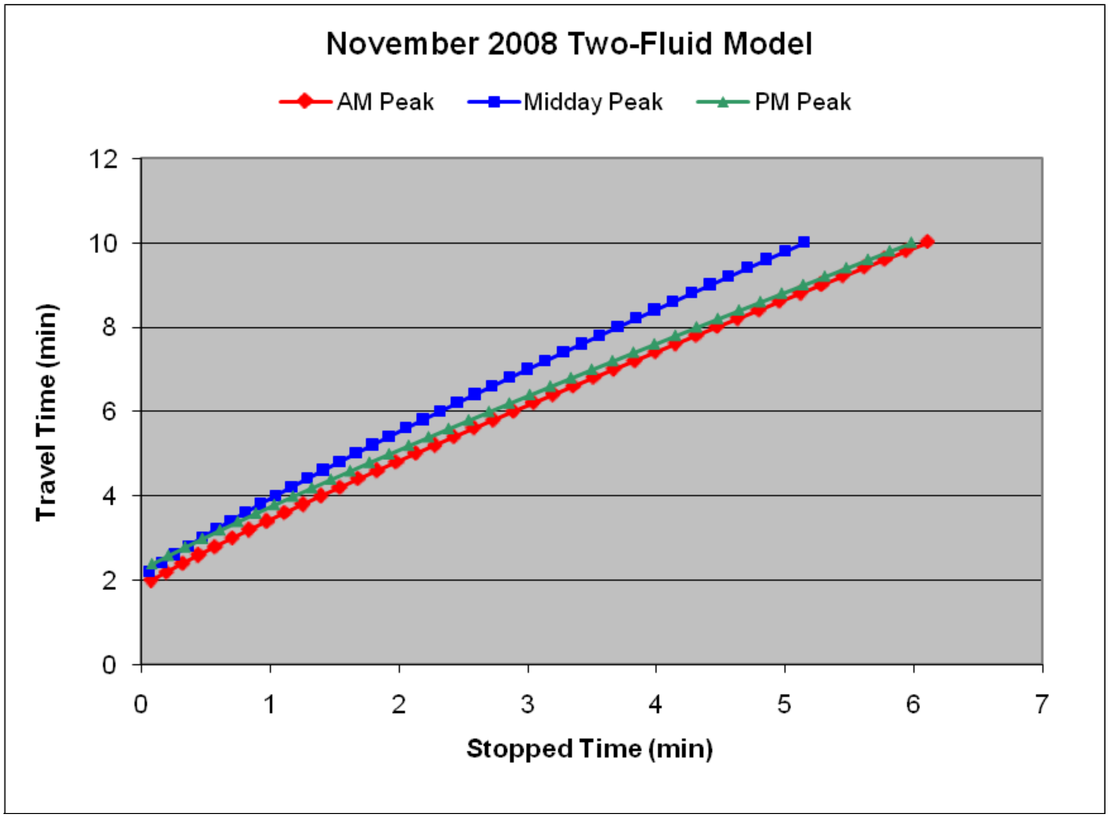

Figure 7: November 2008 Two-Fluid Models

3.3.2: February vs. November Comparison

Once again, the graphs in Figure 7 can be used to perform a visual comparison of the performance of each traffic peak. However, since the two-fluid model from February was also available, additional comparisons could be made between the models of February and November. Any change seen in the two-fluid model would be the result of the completion of the construction work on the downtown network. Figure 8 to Figure 10 show the graphical comparisons of each peak between Febrary and November.

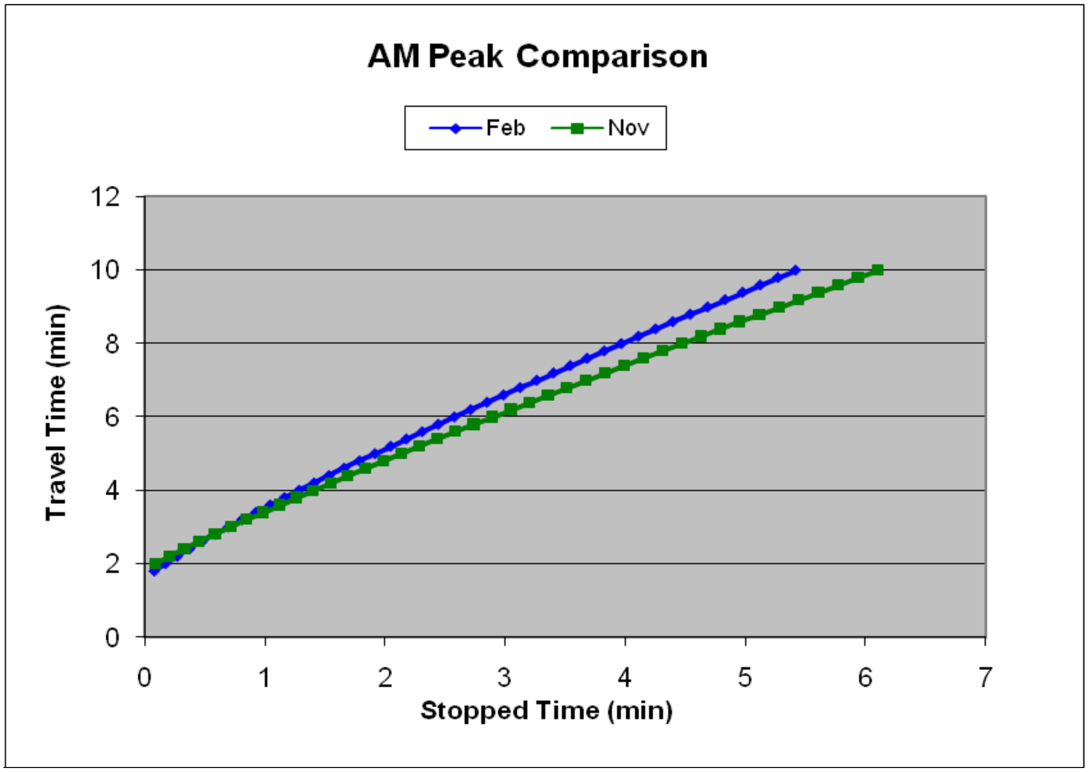

Figure 8: Field Data Two-Fluid Model AM Comparison

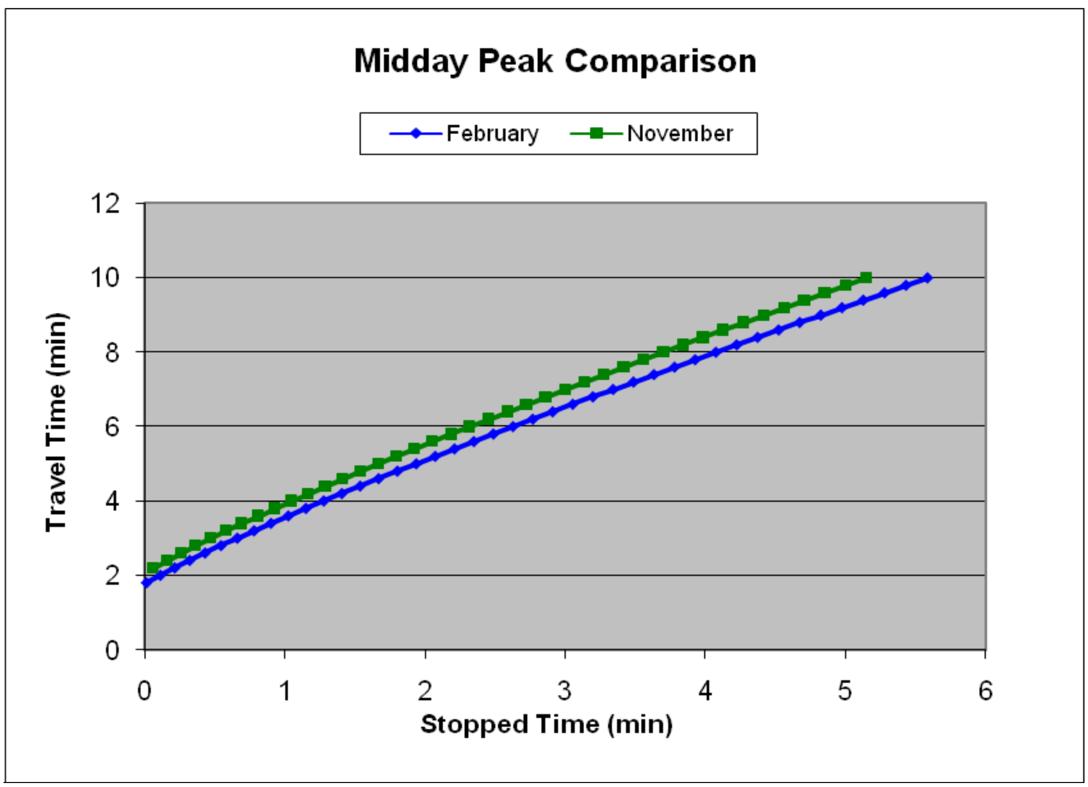

Figure 9: Field Data Two-Fluid Model Midday Comparison

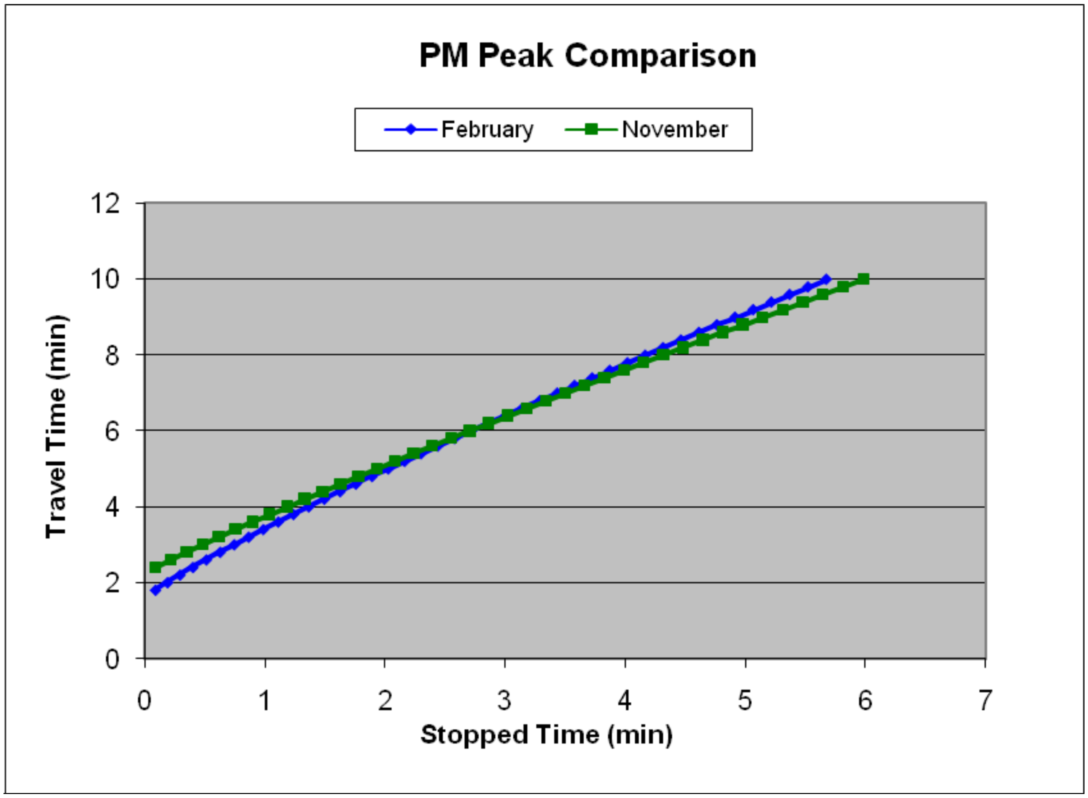

Figure 10: Field Data Two-Fluid Model PM Comparison

According to the above figures, there is a difference between the slopes of the AM and PM peaks for the two months. In both cases, the November network's slope is shallower than the February slope. This indicates that changes made to the network give it the ability to better handle congested conditions. However, in both November networks, the intercept with the vertical axis is higher indicating that under light traffic, the network had higher travel times than those of February. The midday peak is slightly different since the November free flow travel time is higher than February's but the slopes are almost identical meaning that performance during congestion changed very little.

3.4: Statistical Comparison

Even though the graph of the two-fluid model revealed much information about different networks, it was still important to establish if there was a statistically significant difference between the two-fluid models. In order to compare the November field data with the February field data, the "least squares" statistical method was used on the lnTT and lnRT data to calculate the regression terms A and B along with their standard error. This was done as an alternative to obtaining A and B directly from the equations in Figures 4 and 6. Each regression term from the two different field data samples was compared separately using the Student's t-test in the form of Equation 8. For example, the A calculated from the February data was compared with the A calculated from the November data. The null hypothesis, H_0, was that there was no difference between the two data sets. Any difference between the regression terms for each data set would reflect differences between the two-fluid models since the regression terms are used to directly calculate the two-fluid model parameters. Equation 10 shown below was used to calculate the t-statistic which described the difference between the regression terms.

$$T = \frac{\left(\bar{Y}_1 - \bar{Y}_2\right)}{S_p\sqrt{\frac{1}{n_1} + \frac{1}{n_2}}} \tag{8}$$

Recall that the standard error of a sample is defined as follows:

$$SE_x = \frac{S_x}{\sqrt{n_x}} \tag{9}$$

Applying the Equation 9 to Equation 8 yields the Equation 10, which was used for all of the following statistical comparisons.

$$T = \frac{\left(\bar{Y}_1 - \bar{Y}_2\right)}{\sqrt{SE_1^2 + SE_2^2}} \tag{10}$$

With each t-statistic, the corresponding p-value was found which caused either the acceptance or rejection of the null hypothesis. Table 4 to Table 6 shows this statistical comparison in action by comparing the February and November two-fluid models.

Table 4: Statistical Comparison for AM Peak Field Data

	n	ybar	S	SE	t-test	p-value
		Regression Term A				
	n	ybar	S	SE	t-test	p-value
February	88	0.207995	0.671301	0.071561	1.222762	0.226281
November	59	0.343170	0.647223	0.084261		
		Regression Term B				
	n	ybar	S	SE	t-test	p-value
February	88	0.570484	0.3659675	0.039012	-2.04677	0.045144
November	59	0.440450	0.3851539	0.050143		

where: n = sample size
ybar = sample mean
s = sample standard deviation
SE = sample standard error
t-test = probability result of Student's T-test
p-value = significance of the statistical results

Table 5: Statistical Comparison for Midday Peak Field Data

	n	ybar	S	SE	t-test	p-value
		Regression Term A				
	n	ybar	S	SE	t-test	p-value
February	59	0.269913	0.576814	0.075095	0.581491	0.563202
November	57	0.335750	0.639734	0.084735		
		Regression Term B				
	n	ybar	S	SE	t-test	p-value
February	59	0.528721	0.3646598	0.047475	0.175848	0.861036
November	57	0.541284	0.4030597	0.053387		

Table 6: Statistical Comparison for PM Peak Field Data

	n	ybar	s	SE	t-test	p-value
		Regression Term A				
	n	ybar	s	SE	t-test	p-value
February	60	0.223358	0.514403	0.066409	2.806300	0.006748
November	64	0.517996	0.650565	0.081321		
		Regression Term B				
	n	ybar	s	SE	t-test	p-value
February	60	0.539130	0.2740776	0.035383	-2.68284	0.009418
November	64	0.377754	0.3891483	0.048644		

When analyzing the statistical results, a p-value of less than or equal to 0.05 meant that the null hypothesis had to be rejected or that the difference between the regression terms was statistically significant. Applying this criterion to the above tables says that for the AM peak data, term A is not significant while term B is. For the midday peak, the results show that the network models had very similar characteristics which can also be seen in Figure 9. The statistics for the PM peak, on the other hand, show that the February and November models are clearly not similar. With the formulation of the two-fluid models for the February and November traffic peaks complete, the next step was to replicate the network conditions encountered during each round of data collection within a VISSIM network model.

CHAPTER 4: VISSIM NETWORK MODELING

With the February two-fluid model for the real world downtown network formulated, the basis for calibration was established. The next step was the construction of a VISSIM model which, as accurately as possible, duplicated the driving conditions encountered during the data collection. To achieve this, the actual and virtual networks had to match with respect to geometry, signal timings, and volumes. It is important to note that before the modeling took place it was decided that only two traffic peaks would be modeled: the AM and the PM peak. There were two reasons for this. First, there was not enough data available on the volumes of the midday peak and second, the traffic experienced on the midday peak during data collection was not nearly as heavy as for the AM or PM peak which meant that it was not a critical peak to model.

4.1: Synchro Import

There were two viable options available for creating the geometry of the network: create the network from scratch or import portions of the network from other simulation software. The former option was not appealing considering the amount of tedious man hours it would have required simply to create the network geometry. Upon investigation, the latter option turned out to be more viable and was pursued. Importing the network from another program was facilitated by using a model of the downtown network already created for the City of Orlando within the program Synchro 6. Even though Synchro is a macroscopic program designed more to be an optimizer rather than a simulator, it was possible to export the basic network components out

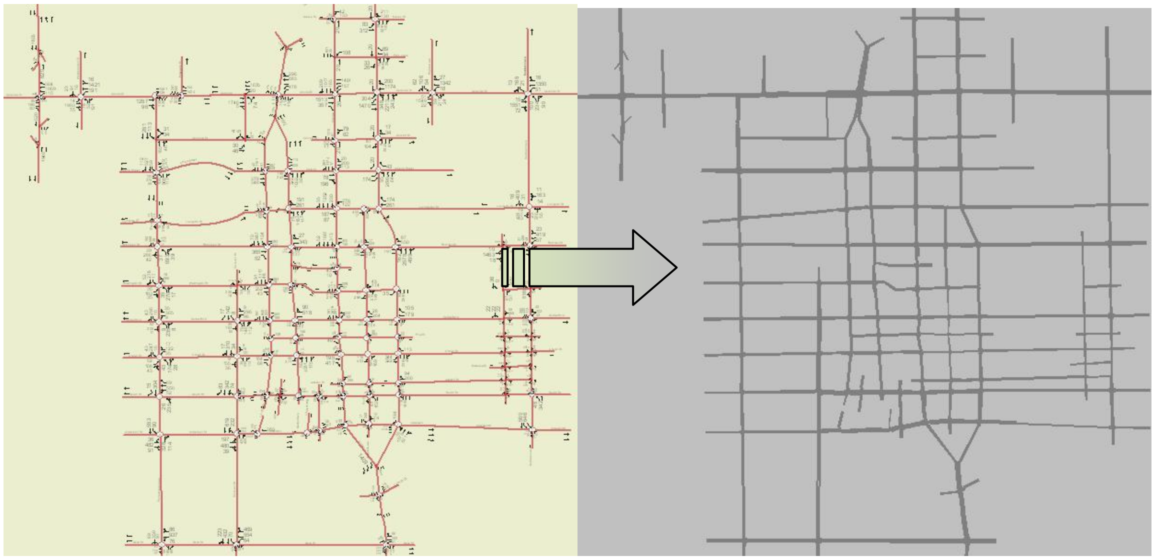

Figure 11: Downtown Network in Synchro (left) and VISSIM (right)

of Synchro and import them into VISSIM. Figure 11 shows the two networks side-by-side. Even though the Synchro import provided an alternative to creating the network from scratch, there were still many details to work out regarding the network's geometry and other simulation elements. For instance, the Synchro network used for the import was intended to be a model for the year 2015 and included certain changes the city had wanted to consider. The city provided a list outlining several changes that had to be made to convert the network to the February 2008 conditions.

In addition to network changes, the Synchro import also had functional difficulties at intersections which produced unrealistic traffic patterns and behavior during test simulations. Since this problem was simulation-wide, the solution used was to systematically go to each intersection and run through the simulation network elements to ensure realistic activity. This process was called "proofing the simulation" and used the following procedure.

- Check the number of lanes on each approach and each turning movement
- Adjust turn radii to follow realistic paths
- Install crosswalks where none exist

- Check lane markings
- Insert vehicle inputs where applicable
- Check routing decisions to ensure there are no broken connections
- Set desired speed decisions to the current speed limit
- Install and/or reposition reduced speed areas on intersection turning movements
- Install stop signs for stop control or right turn on red
- Check yield rules to ensure proper right-of-way is given
- Install and/or reposition signal heads

The most drastic example of the use of this process was at the interchange of I-4 and Colonial Dr. Figure 12 shows the interchange generated by the Synchro import and the final result.

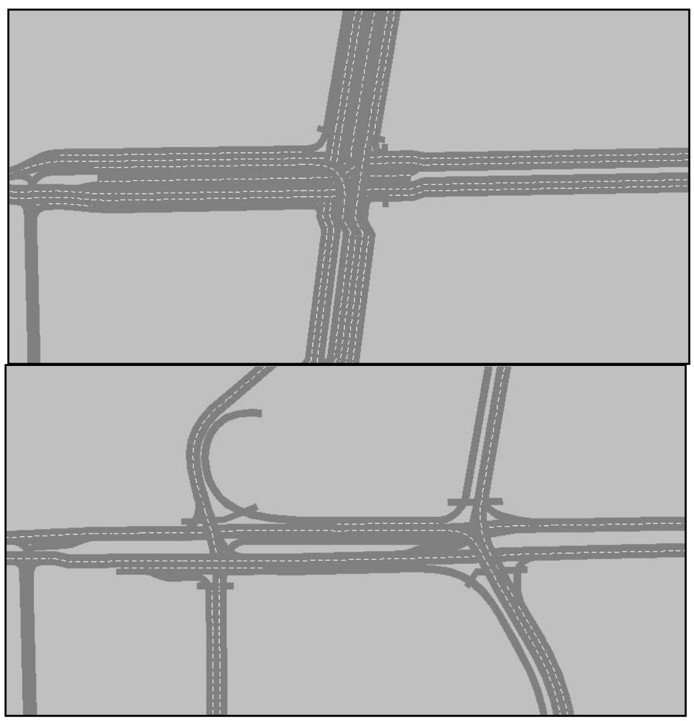

Figure 12: Example of Intersection "Proofing": Synchro Import (top) Final Geometry (bottom)

Along with changes that had to be made to individual intersections, the original Synchro import did not include all portions of the project area. Two large corridors that were missing from the import were Orange Blossom Trail (OBT) and Westmoreland Ave. Fortunately, a

Synchro network of OBT had also been created to simulate the 2008 conditions. This network was imported into its own VISSIM file and then added to the main network file using the "Read Additionally" tool in VISSIM. From there it was a simple task to integrate OBT into the network and perform the same "proofing" of each intersection that was done to the rest of the network. Figure 13 shows the OBT corridor before and after the import.

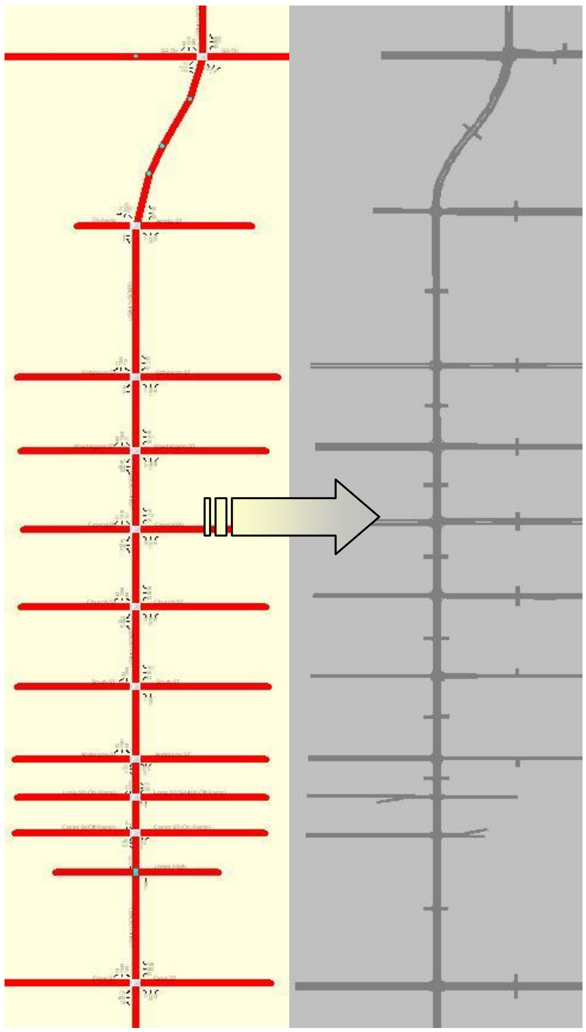

Figure 13: Orange Blossom Trail in Synchro (left) and VISSIM (right)

Unfortunately, a Synchro file did not exist for Westmoreland Ave. which meant that it had to be coded into the model from scratch. Another alternative considered was to simply not include Westmoreland in the network. However, this was deemed to be shortsighted since the many planned and current developments in the project area indicate that Orlando's downtown is expanding in the direction of Westmoreland and to exclude Westmoreland's impact to traffic and the two-fluid model would be negligent. Also, recall that in Table 1, one of the factors affecting the two-fluid parameters is signal density. Ignoring Westmoreland would mean ignoring an entire signalized corridor since all of the intersections of Westmoreland with other roadways in the network are signalized. Such an action would have produced a two-fluid model that did not accurately reflect the network. Therefore, it was decided to enter Westmoreland into the network from scratch. The "proofing" procedure was used as with the other intersections on the network with one additional step at the beginning: insert links and connectors for all approaches and intersection movements. With the geometry and simulation elements set, the next step was to adjust the signal timings and volumes to match the AM and PM peaks.

4.2: Signal Timing Data

Within the project area, a total of 104 signals were modeled with almost every intersection being signalized. Recall that in Table 1, the two-fluid model parameters are influenced by the presence of and timing of traffic signals on the network. Since the signals in the network used fixed time operation and the density remained the same between the AM and PM peaks, only two of the factors listed in Table 1 applied to this network: cycle length and fraction of signal approaches with progression. The city provided the signal timings as well as offset times and patterns for the AM and PM peaks.

In order for the signal data to be integrated into the simulation, each set of signal heads at a given intersection was assigned a signal controller number. Most of these numbers and controllers were imported from the node numbers used in the original Synchro file. The signal timing data was entered from within the "Edit Controllers" window in VISSIM using the NEMA controller software included with VISSIM 4.3. The NEMA software provides the option of using a “standard editor” or a “simple editor”. The standard editor provides all the capabilities of the typical NEMA controller but is very complex and requires proficiency in the use of NEMA software. The simple editor, on the other hand, is a more user friendly version of the software and is suited to most signalized intersection setups (i.e. four approaches, left turn phases, offsets, fixed and actuated phases, etc.). Since most of the intersections in the network are four leg and/or two to four phase signals, the simple editor was selected for use throughout the network. If a case ever presented itself where the simple editor was insufficient, the signal could be switched to the standard editor to allow a more customized timing. Figure 14 shows the simple editor window for a typical intersection.

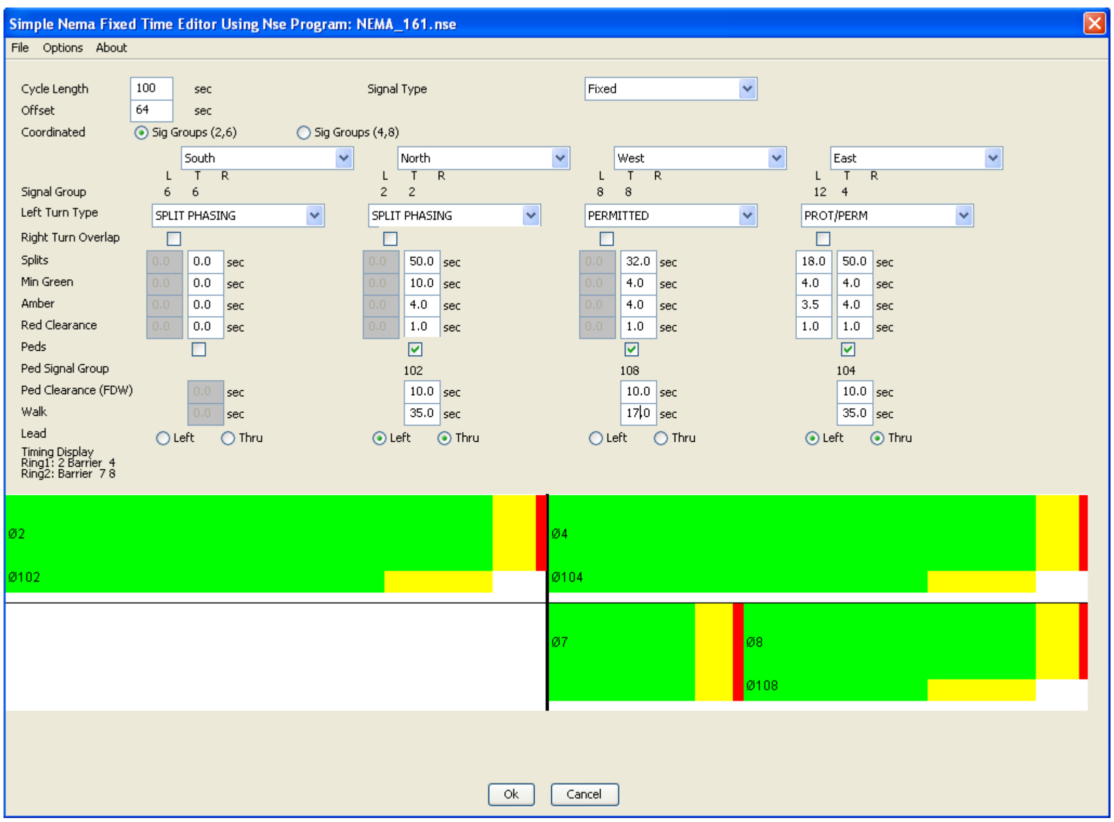

Figure 14: The Simple NEMA Editor Window

As with the intersection “proofing”, each intersection’s signal timing was checked to ensure it matched the data provided by the city. The procedure used was as follows:

- Using the signal controller spreadsheet provided by the city, check the minimum green, yellow, all red, and pedestrian timings.
- Determine the section of downtown the intersection is located in and highlight that section on the coordination planning spreadsheet.
- Using the coordination planning spreadsheet also provided by the city, set the offsets, phasing order, and split times.
- Install any missing signal heads at the intersection and ensure the existing ones are set to the proper phasing.

With the signal timings set to match the conditions of either the AM or PM peak, the final step before simulations could be run was to insert the proper volumes into the simulation.

4.3: Volume Data

Before the VISSIM model could be calibrated, the volumes experienced by the network on or close to the day of data collection had to be entered in. Recall that microsimulations usually employ O-D matrices to accomplish this task as was done in Jha et al. [10] and Toledo et al. [11]. However, since the two-fluid model is macroscopic in nature, dynamic route assignment governed by a full O-D matrix was deemed unnecessary. As an alternative, it was decided to incorporate the latest volume and turning movement ratio data with the static route decision tool within VISSIM.

The procedure of determining the network volumes involved assembling all the available volume data into a single spreadsheet, coding in entrance and egress points or "driveways" at mid-block locations, and updating the routing information. The first step in entering the counts into the VISSIM network was to determine what information was available to estimate the traffic volumes that occurred during the data collection. Unfortunately, there was no single source where all turning movement and volume data could be collected for the network which meant multiple sources had to be utilized. Information available included 2008 Synchro files for the downtown core and OBT, 2007/08 counts at mid-block locations throughout south downtown in PDF files, a 2015 Synchro file with PM volumes covering the entire network, and paper printouts showing the 2001 and 2020, AM and PM volumes for most of the network. Before the counts were coded into VISSIM, all the available information was compiled into one

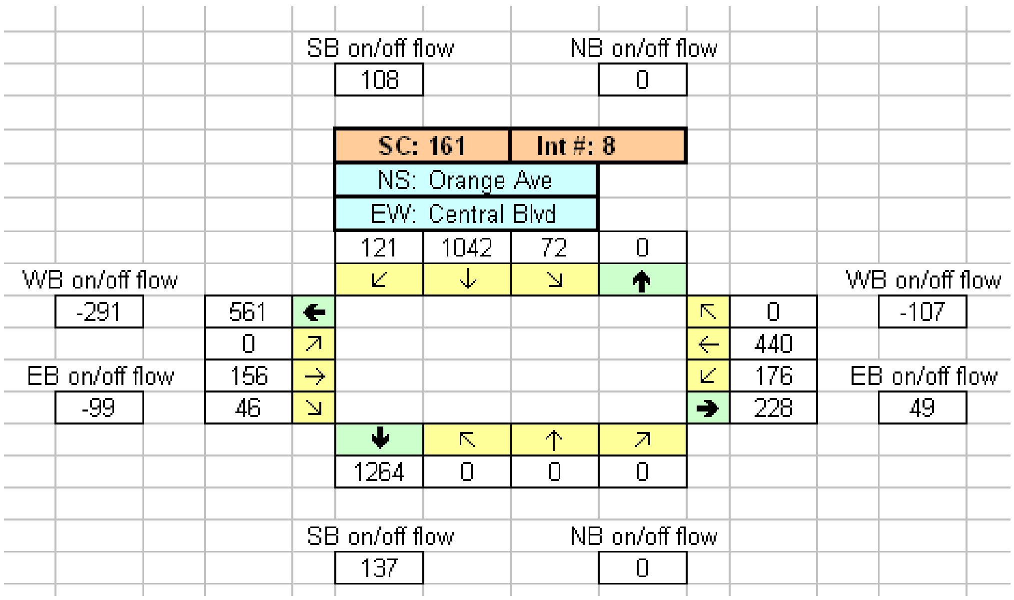

Figure 15: Traffic Volume Spreadsheet Typical Intersection

comprehensive location. The known counts were entered into a spreadsheet which showed each intersection on the network as four approaches as shown in Figure 15. Between each of these intersections, the volume difference between the upstream intersection departure and downstream intersection approach was calculated. A positive value indicated a volume that should enter the road before the next intersection while a negative value indicated a volume that should depart the road.

In order to provide an accurate picture of the traffic volumes, the most accurate data was entered in first followed by the next best data and so on. The procedure used for inserting the traffic counts is shown below:

- The volumes from the 2008 Synchro files were entered into the turning movement cells at each intersection.
- The NS or EW mid-block counts from the 2007/08 PDF files were applied to the 2015 turning movement count (TMC) ratios to distribute the volumes at the downstream intersections.
- Adjust the TMCs as needed to match changes to the 2008 network. (i.e. Anderson St overpass closure.)
- For boundary approaches, the 2015 volumes were reduced assuming a 3% reduction in traffic volume per year. Since 2008 is seven years prior to 2015, 21% reduction was applied to the 2008 volumes with Equation 11.

$$V_{2008} = V_{2015} \text{ x } (100/121) \qquad (11)$$

It should be noted that for the PDF counts, the maximum volume used had to have occurred during or within an hour of the data collection times (AM Peak: 7am-9am, PM Peak: 5pm-7pm). Also, since there was no available data for Westmoreland Dr, that road was assumed to have the same TMC ratios as Parramore Ave since the two streets travel through similar environments and have similar cross sectional characteristics. Another note is that there was a difference in procedure with the AM network. Since there was no AM 2015 Synchro network available, the TMC ratios from the 2020 printout were used for most of the network with the 2001 printout used where network geometry had been altered. For the remaining area not covered by the printouts, the PM 2015 Synchro file was used for its TMC ratios.

After all applicable PDF and Synchro volumes were inputted into the spreadsheet, several intersections were still without approach information. For these incomplete approaches, an iterative procedure was used to fill in the holes. This procedure starting at the western end of the network and was performed block by block. Any volume found feeding into an intersection approach with no data entered was distributed using the 2015 TMC ratios and entered into the empty cells so the mid-block driveway had no volume. Care had to be taken to account for one-way streets or road closures when performing this distribution.

The reason this process required iterations was that once a mid-block driveway was set to zero, the balance would be upset if any approach that fed into the balanced segment was modified. The iteration was monitored with the following procedure.

- The zeroed approach was marked with a "\" underneath the driveway volume to keep track of which segments had been zeroed.
- Moving from west to east, the entire network was filled in.
- Then all the driveways with the "\" under them were revisited, rebalanced, and marked with a second "\".
- A volume close to zero, not exactly zero, for each driveway was the goal. Therefore, iteration for a given segment was not performed when the difference was less than 10% of the volume entering the upstream intersection. Such segments were marked with a "@" to show that the volume driveway volume had been locked in.

Along with simply filling in the holes of missing data, it was discovered that areas of the network with known volumes had issues of their own. Through trial simulations, it was found that large exiting volumes at midblock driveways were causing unrealistic weaving conditions and not allowing the proper volume to flow through. The solution developed was to provide a criteria for the mid block driveway volumes.

- Start with the raw driveway volumes from the volume spreadsheet.
- If there are any driveways with an entrance or exit volume >100,
  - Determine from existing field conditions and land usage if such a traffic generator or destination exists.
  - If one does not, reduce the volume entering or exiting to 0, consider it as volume traveling to the next intersection, and distribute the volume using known TMC ratios.
  - If one does exist but does not appear to be able to handle the traffic, reduce the volume to between 100 and 300 based on the size of the generator/destination and perform the same procedure for the extra volume.
  - If one does exist and it does appear to be able to handle the volume (i.e. a freeway ramp), make geometric changes to allow the volume to realistically enter or exit the network.

An example of improving the geometry of a midblock driveway can be seen in Figure 16 which shows the driveway on Orange Ave between Anderson St and Lake Lucerne Cir. The original driveway configurations for both northbound and southbound were incapable of handling the volumes assigned in the volume sheet but the large volume made sense because of the SR-408 on ramp located on that segment. This prompted the geometric changes shown. This also, included the insertion of the signal associated with the on ramp and resulted in a simulation which better reflected actual network conditions.

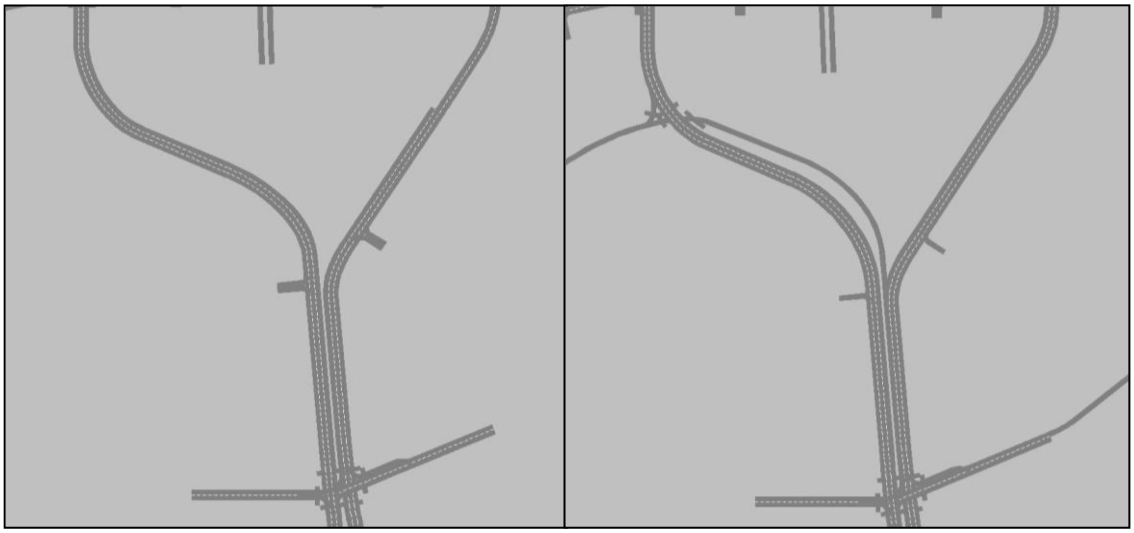

Figure 16: Geometric Enhancements to Midblock Driveways

The determination of these new driveway volumes was also part of the iterative process but only applied to areas of the network where the volumes were known from more reliable sources. Only two iterations of the entire network were necessary to meet the conditions above.

With the turning volumes calculated and the spreadsheet filled in, the next step was the coding of the mid-block driveways and the network routing decisions in VISSIM to reflect the volume sheet using the procedure shown below.

- A N/S road was selected and a driveway was placed at each mid-block point for each direction. A driveway consisted of a one lane exit and entrance and mimicked the layout of a standard two-way, right-in-right-out driveway.
- Driveways were placed at each mid-block point for the E/W segments adjacent to the selected N/S road.
- Driveway placement included:
    - Links, connectors, reduced speed areas, priority rules, and stop signs.
- Once the driveways were placed on the selected road, the volume spreadsheet was consulted and the volumes were placed accordingly. If the spreadsheet showed a

negative mid-block flow, the driveway was considered a sink and the upstream route decision was used to send the appropriate volume into the driveway. If the mid-block volume was positive, the driveway was considered a source and the driveway input link was given a vehicle input with the correct volume.

Figure 17 shows a typical driveway as it appeared in the network. For all driveways, if there was traffic flowing in, no traffic would flow out and vice versa. In some cases, the placement of a driveway was not practical or realistic. Network links in areas that have no driveways in real life (i.e. OBT underneath SR-408 or areas running through construction zones) were not given a driveway in the network. Such a situation is shown in Figure 18. Also, for links that were extremely short (i.e. Rosalind Ave between Pine St and Central Blvd) the network entrance segment of the driveway was placed before the network exit segment to give vehicles more time to make necessary maneuvers.

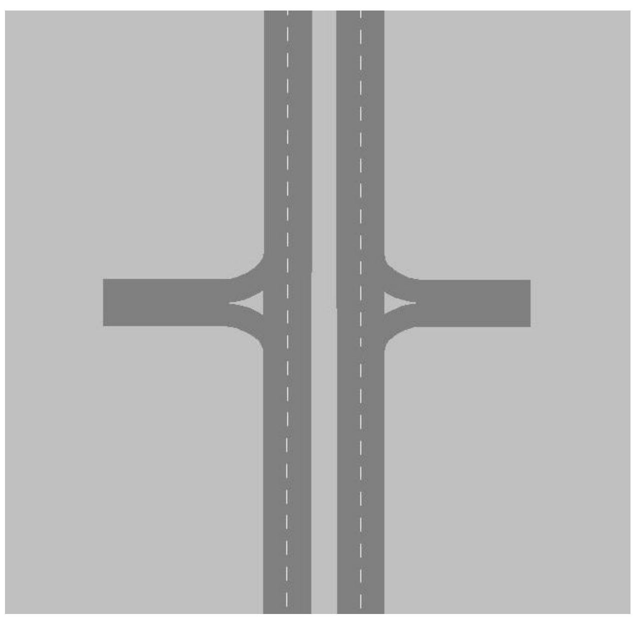
Figure 17: Typical Midblock Driveway

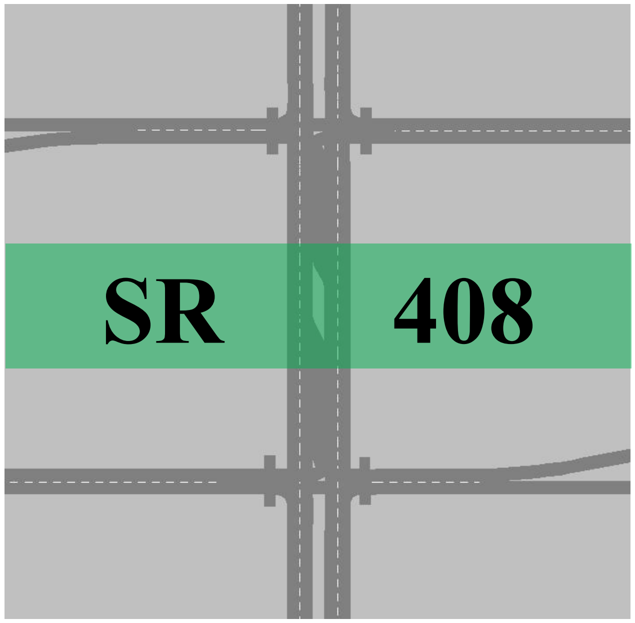

Figure 18: An Example of an Omitted Driveway

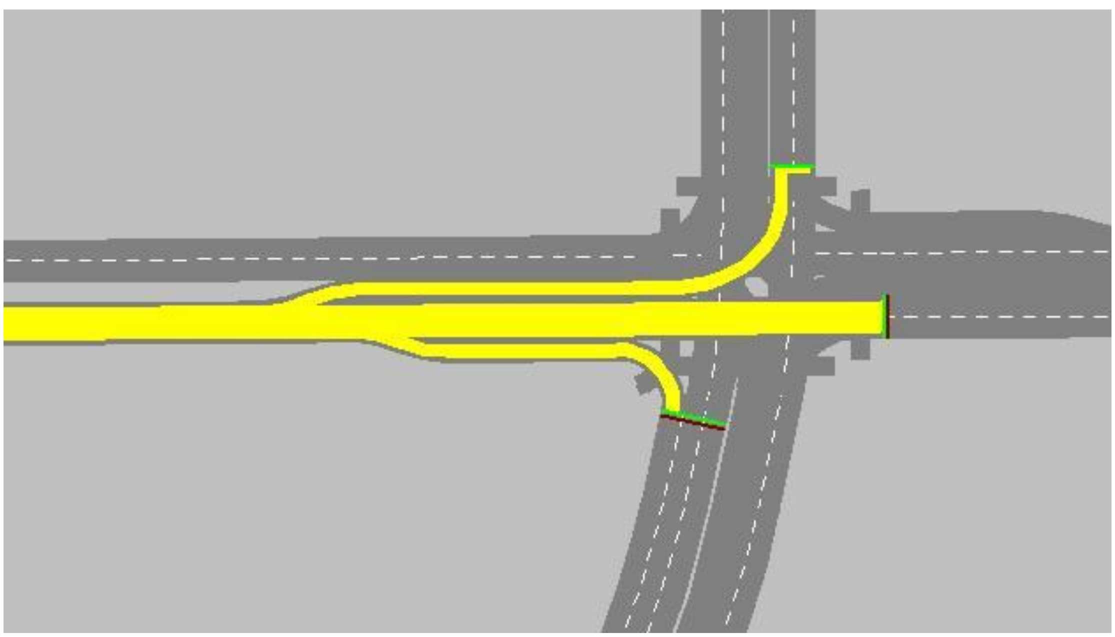
Figure 19: Route Decision Example

Once all the driveways were coded, the turning movement volumes in the spreadsheet were entered into the routing decisions. Unless the approach came from the network boundary, each approach had two route decision points: one immediately after the upstream intersection and another on the inflow segment of the driveway. Figure 19 shows the routing situation at a typical intersection. In some cases, the close proximity of a series of intersections coupled with heavy through and turning volumes caused unrealistic congestion on the network due to traffic weaving. When this occurred, one routing decision directing mainline traffic was set to span multiple intersections which assigned vehicles their route earlier allowing them more time to make the necessary lane changes. In order for these routing combinations like the one shown in Figure 20 to work, they also required that the “lane change distance” for vehicles wishing to use a certain connector had be extended so drivers would utilize the extra distance.

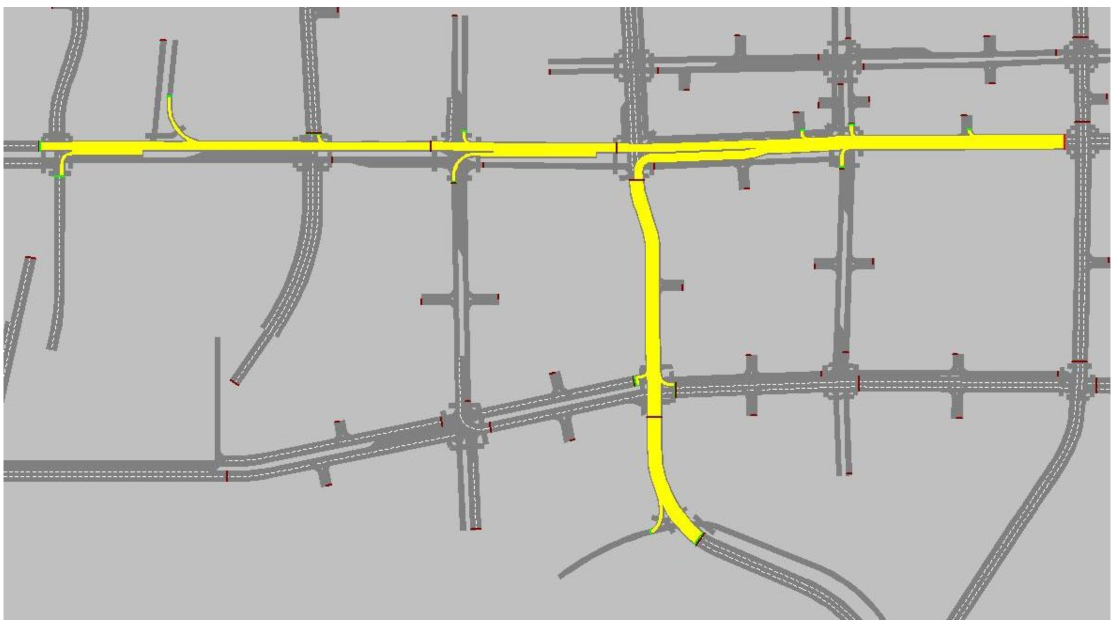

Figure 20: Intersection Routing Combinations

Once the routing decisions were entered, the coding of the current traffic volumes into the VISSIM network was complete. These same procedures were used for both the AM and PM peak networks after which the calibration of the VISSIM network was performed.

CHAPTER 5: CALIBRATION AND VALIDATION

5.1: VISSIM Network Calibration

Calibration of the complete VISSIM network of the February 2008 conditions involved manipulation of select driving behavior parameters within the VISSIM simulator. The process utilized was a trial and error method whereby a simulation was performed, the two-fluid model was generated, and the field two-fluid model was compared with the one generated in VISSIM. If the two models were not statistically similar, then the behavior parameters were modified and the process repeated. The following sections describe the process in more detail.

5.1.1: Driving Behavior Parameters

Within VISSIM there are numerous driving behavior parameters that can be adjusted to customize a simulation. These parameters affect behavior such as vehicle following, lane change, lateral spacing, and signal observance. For the purposes of this project, two parameters under the vehicle following category, shown in Figure 21, were modified. These parameters were the average standstill distance and the look-ahead distance for the car following model. Only these two parameters were selected because they affect the aggressiveness of the drivers on the network. For example, the average standstill distance controls how much space is left between vehicles in a queue on average. Aggressive drivers would have a lower value for this behavior. Also, for the look-ahead distance, it affects how far ahead the drivers look and prepare for conditions ahead. Again, the lower the value, the more aggressive the drivers are.

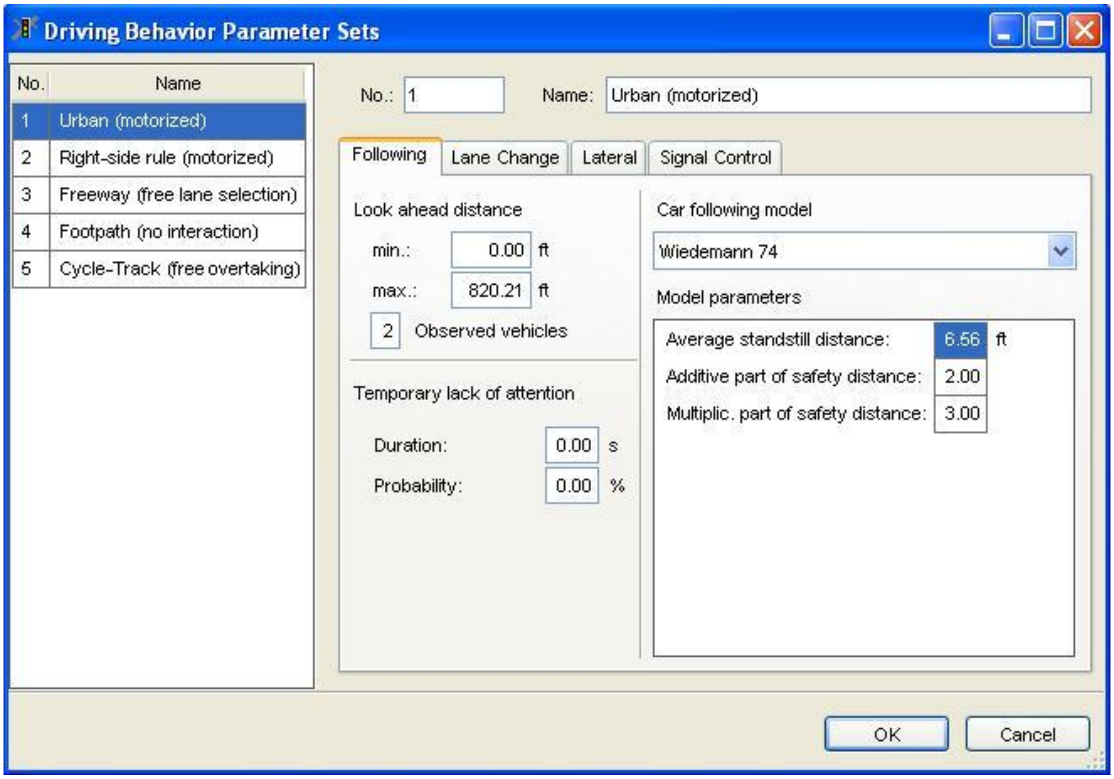

Figure 21: Following Behavior Parameters in VISSIM

5.1.2: Vehicle Record Data

With the behavior parameters selected, the next task was to set up a means of obtaining the data necessary to generate the two-fluid model from the VISSIM simulation. VISSIM has a large variety of ways to collect almost any type of traffic, roadway, and even emission data but for this project, the goal was to find a data collection method that imitated the chase car methodology used for data collection on the physical network. The vehicle record tool was selected as the best suited to achieve the desired similarity since data is collected about the individual vehicles on the network. Figure 22 shows the evaluation and configuration window where selection of the data to be collected is done. In order to provide the same data collected in the field, the parameter selected were vehicle number, vehicle length, simulation time, total path distance, speed (mph), and the number of stops. The filter tool attached to the vehicle record selection was used to dictate that all the parameters listed would be collected for every vehicle on the network every 0.1 simulation seconds. Because of the large amount of data this would result in, data collection was limited to a 130 second window beginning at 1800 seconds into the simulation. After the simulation was complete, VISSIM would automatically create a text file containing the vehicle record data. The next step was processing the data to acquire the needed information.

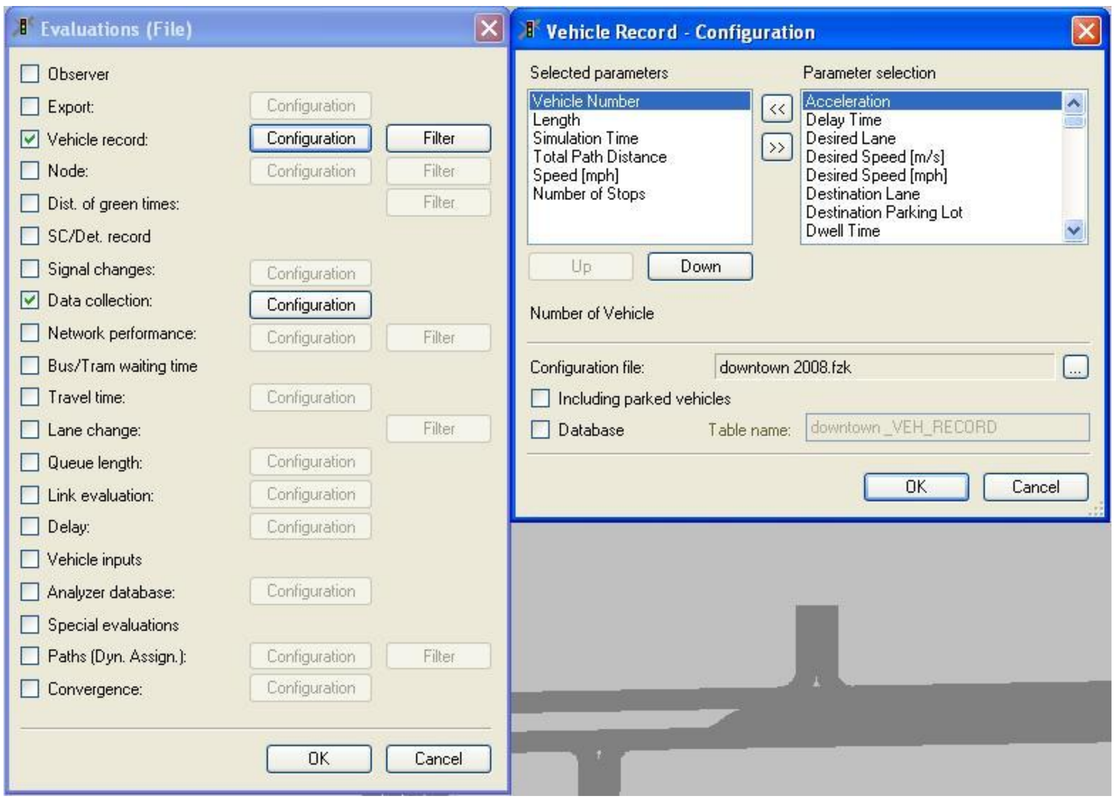

Figure 22: Vehicle Record Configuration Window

5.1.3: Matlab Analysis and Statistical Comparison

As mentioned before, the vehicle record tool collected the outlined parameters for each vehicle ten times each simulation second. Depending on the network being run, there were on average 3000-5000 vehicles on the network at any given time. For a data collection period of 130 simulation seconds, this results in anywhere from 3.9-6.5 million points of data for each file. This led to text files with sizes ranging from 20-30 MB. With this much data available, manual analysis was out of the question. Therefore, as a means of speeding up the data mining process, a Matlab program, shown in Figure 23 was written which sifted through each text file and produced 100 data points for random vehicles over a time period of 120 simulation seconds to imitate the two-minute method of data collection. Each data point provided by the Matlab program contained the vehicle number, travel time, stopped time, distance traveled, and number of stops over the course of the two minute observation period. The reason a 130 second period was used within VISSIM when only 120 second periods were desired was to provide a 10 second cushion so the vehicle trips produced using Matlab would not have to fall exactly within a strict 120 second time period. For the calibration, only one VISSIM run with one seed number was needed since random selection of vehicles was achieve by the Matlab program and the 100 data points produced by Matlab was deemed to be enough to perform calibration.

With 100 data points from vehicles on the simulated network defined, the two-fluid model for the specific calibration parameters was generated. In order to compare the simulation with the field, the "least squares" statistical method was used on the ln*TT* and ln*RT* data as in section 3.4 to calculate the terms A and B used in Equations 5 and 6 which also calculated the standard error for each term. Once the "least squares" method was applied to the field data and VISSIM data, the statistical t-test was performed and the p-value was calculated which provided a statistical comparison of the terms A and B for each data set. For the purpose of calibration the goal was for the p-value not only to be above 0.05, but to be as high as possible so as to increase the confidence percentage with which it could be said that the two-fluid models were similar. For example, a p-value of 0.63 meant that there is a 63% probability that the two-fluid models are statistically similar. A standard similar to the one cited in Dowling et al. [9] was used which called for the statistical comparison to be accepted only if the p-value was greater than 0.85. This statistical comparison was applied to the Matlab results for each set of driving behavior parameters. Since the defaults parameters yielded a model with too low of a confidence level, the behavior parameters were adjusted slightly and the process was repeated. Figure 24 presents a flowchart of the calibration process.

```
clear all;
m=dlmread('data1.txt',';');
% [col, row]=size(m)
a=m;
j=1;
while j<101
    k=1;
    veh_no=a(k,1);
    p=[];
    q=[];
    b=[];
    invalid=[];
    [p,q]=find(a==veh_no);
    invalid=find(q>1);
    b=[p,q];
    [i,c]=size(invalid);
    while i>0
        b(invalid(i),:)=[];
        i=i-1;
    end
    [r,c]=size(b);
    if (r>=120)
        TT=0;
        ST=0;
        dist=0;
        stops=0;
        for iter=1:120
            TT=TT+1;
            stops=stops+a(b(iter,1),6);
            if (a(b(iter,1),5)==0)
                ST=ST+1;
            end
        end
        result(j,:)=[veh_no, TT, ST, a(b(120,1),4)-a(b(1,1),4), stops];
        j=j+1
    end
    for iter2=1:r
        a(b(r-iter2+1,1),:)=[];
    end
end
```

Figure 23: Matlab Program used for Vehicle Record Data Processing

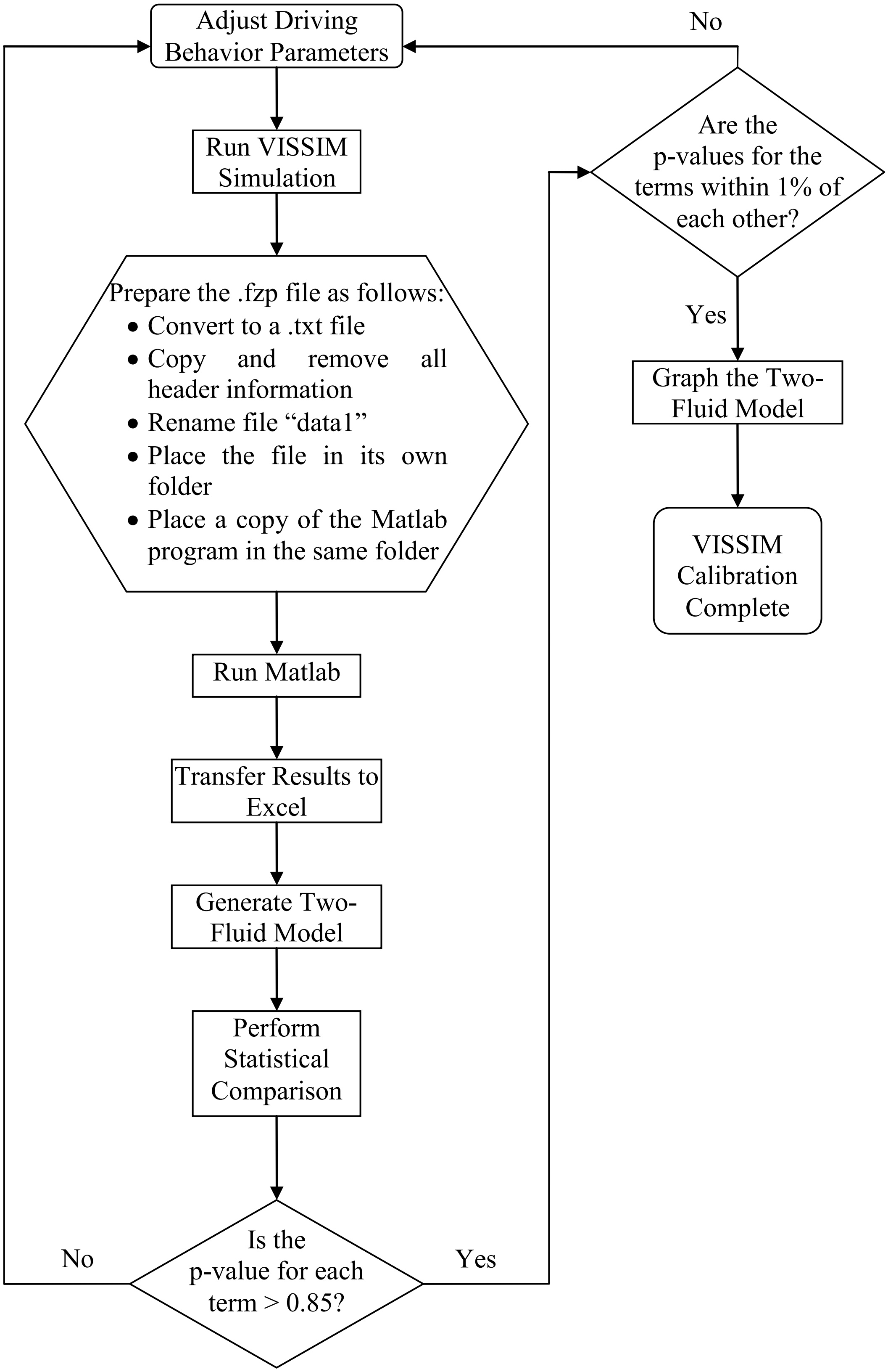

Figure 24: Calibration Process Flowchart

5.1.4: Simulation Two-Fluid Model

In the end, the calibration of the two-fluid model for the AM peak was achieved with a look-ahead distance of 812.01ft and an average stand-still distance of 6.65 ft with rest of the variables kept at the default levels. As shown in Table 7, it was observed that the two-fluid models for VISSIM and the field were not different at a confidence of 87%. The calibration iterations were stopped at 87% because the confidence was over 85% and confidence for both terms A and B were within 1% of each other. Graphical representations of the AM peak two-fluid models are shown in Figure 25.

Table 7: Statistical Comparison for AM Peak Calibration

		Regression Term A				
	n	ybar	s	SE	t-test	p-value
VISSIM	100	0.191130	0.643541	0.075069	0.162666	0.871159
Field	87	0.208000	0.667467	0.071560		
		Regression Term B				
	n	ybar	s	SE	t-test	p-value
VISSIM	100	0.579362	0.3849823	0.038498	-0.162053	0.87164
Field	87	0.570480	0.3638611	0.039010		

where: n = sample size
ybar = sample mean
s = sample standard deviation
SE = sample standard error
t-test = probability result of Student's T-test
p-value = significance of the statistical results

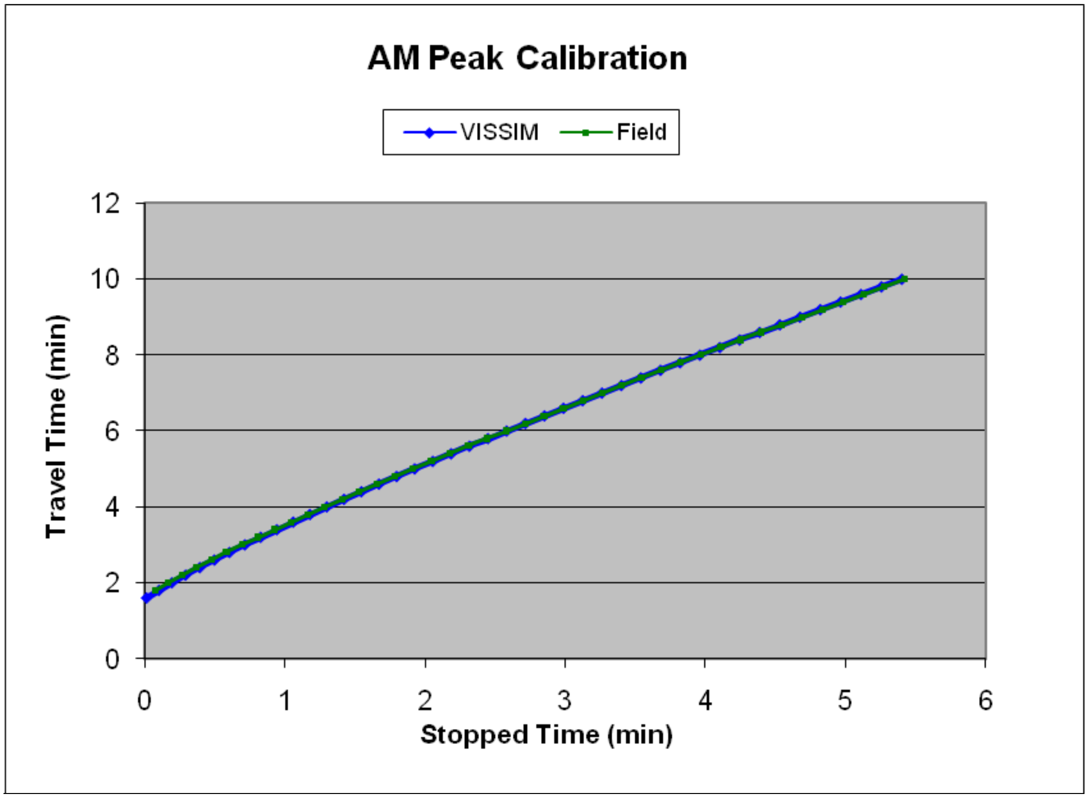

Figure 25: Calibrated Two-Fluid Model for the AM Peak Network

For the PM Peak, the calibration was achieved with a look-ahead distance of 812.01ft and an average stand-still distance of 6.89 ft with rest of the variables kept at default levels. Table 8 shows that the two-fluid models for VISSIM and the field were not statistically different at a confidence of 88%. Once again, the iterations were ceased at 88% because the confidence was over 85% and confidence for both terms A and B were within 1% of each other. Graphical representations of the PM peak two-fluid models are shown in Figure 26.

Table 8: Statistical Comparison for PM Peak Calibration

		Regression Term A				
	n	ybar	s	SE	t-test	p-value
VISSIM	100	0.237016	0.643540	0.064354	-0.147671	0.883106
Field	59	0.223360	0.510105	0.066410		
		Regression Term B				
	n	ybar	s	SE	t-test	p-value
VISSIM	100	0.531799	0.338930	0.033893	0.14963	0.881568
Field	59	0.539130	0.271759	0.035380		

where: n = sample size
ybar = sample mean
s = sample standard deviation
SE = sample standard error
t-test = probability result of Student's T-test
p-value = significance of the statistical results

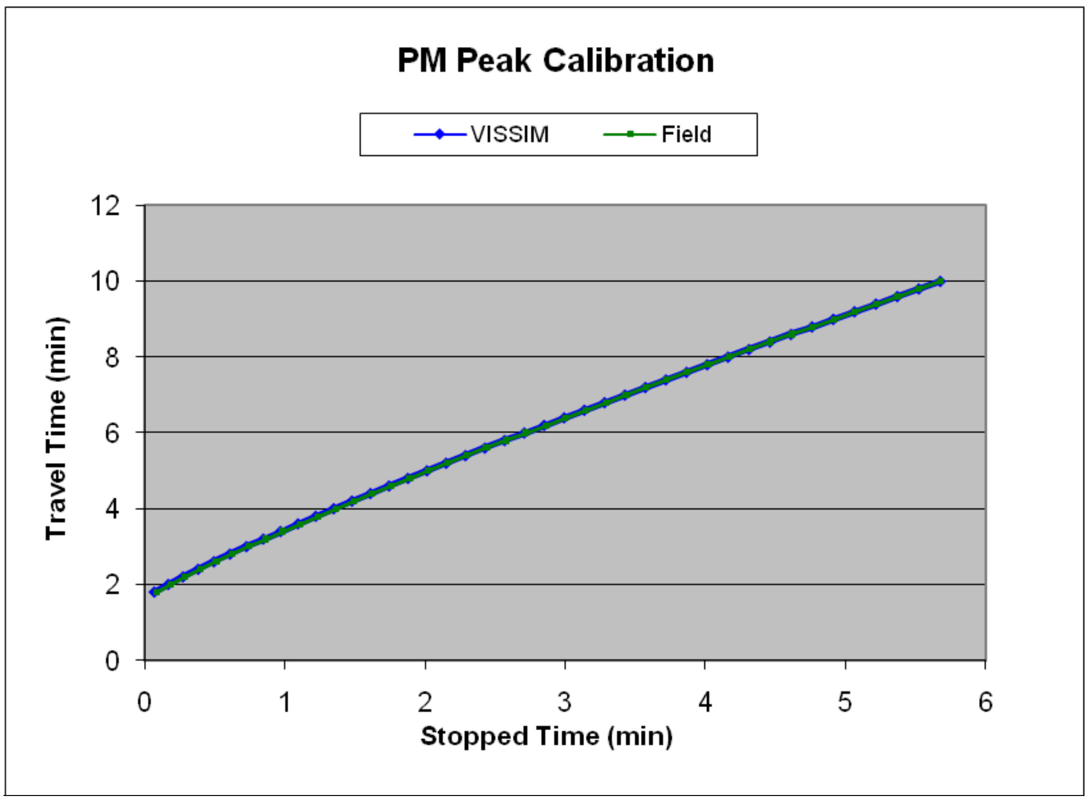

Figure 26: Calibrated Two-Fluid Model for the PM Peak Network

5.2: VISSIM Network Validation

Even though the calibration process produced a VISSIM simulation which was statistically similar to the field network, the true test would be to see if the similarity was maintained with a new set of field data from a downtown network with several geometric changes and an updated VISSIM network reflecting those changes. This process would ultimately result in the validation of the VISSIM network and justify the usage of the simulation to perform comparisons on different scenarios. The data collection which occurred in November was used to create the field two-fluid model for validation purposes. However, before the two-fluid model could be generated from VISSIM, the simulation network had to first be updated to reflect changes that had occurred on the network between February and November.

5.2.1: Network Changes from February to November

In February of 2008 when the first round of data collection occurred, there was a considerable amount of construction on Anderson St. and South St. between Division Ave. and Rosalind Ave. due to an upgrade of the I-4 and SR-408 interchange. Figure 27 shows two aerial pictures of the heaviest area of construction taken in February and August. The construction had resulted in the closure of some roadways and the narrowing of others. However, by November, all lanes had been reopened and only one road segment was closed (Hughey Ave. between Church St. and South St.). All these changes had to be made to the VISSIM network. Figure 28 shows a comparison of the February VISSIM network with the November VISSIM network. There were additional alterations, but Figure 28 presents the highest concentration of changes.

Figure 27: Downtown Construction - February (left) and August (right) (trans4mation.org)

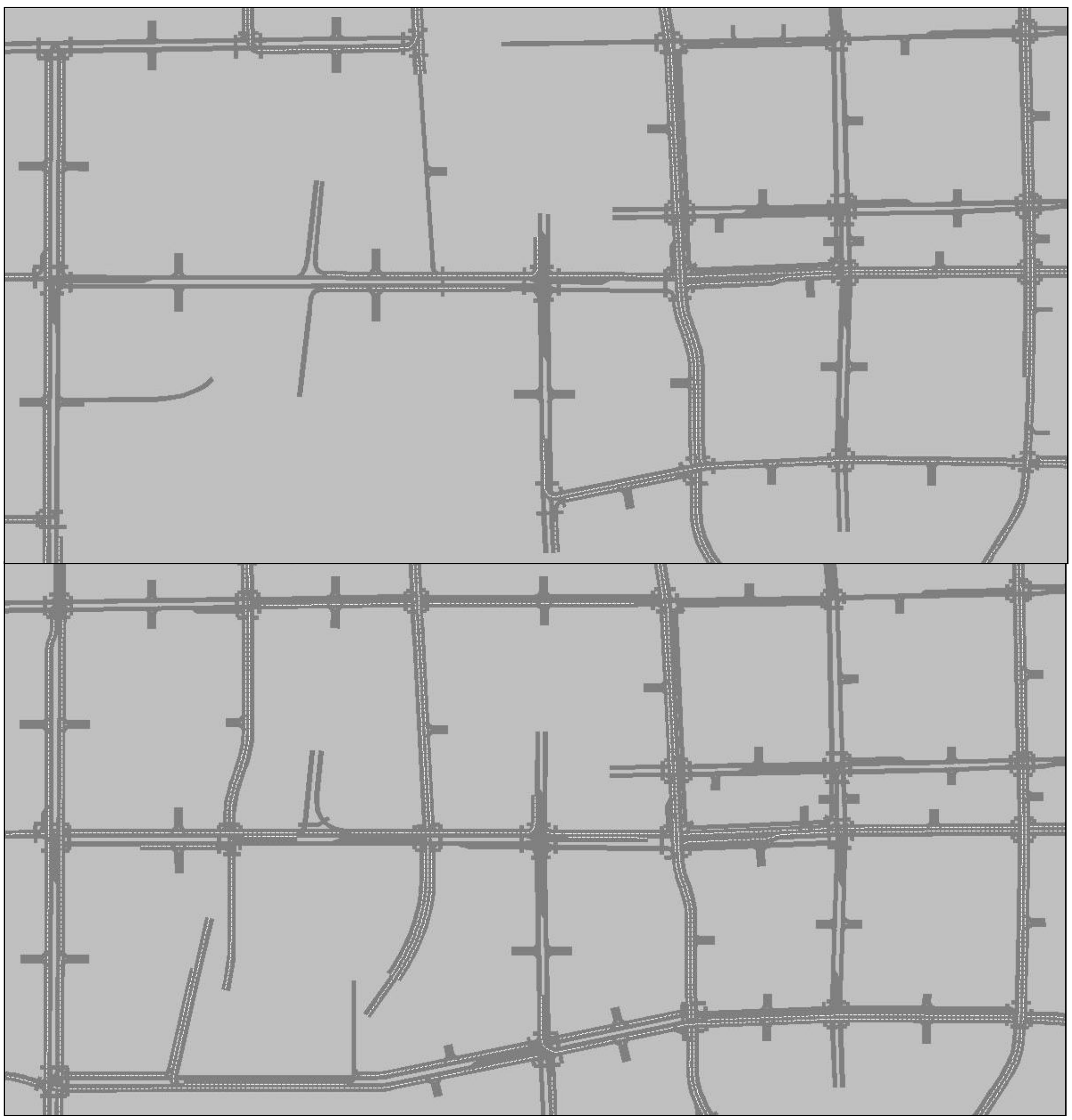

Figure 28: VISSIM Network Changes - February (top) to November (bottom)

In addition to geometric changes, signal timings had to be updated on Anderson St. and South St. between Division Ave. and Rosalind Ave. This new signal information was provided by the city in a Synchro file and reflected the addition of the new lanes and the reconfiguration of the I-4 on and off ramps.

5.2.2: Statistical Comparison and the Two-Fluid Model

Once the VISSIM network had been updated to reflect the changes on the physical network, data collection for the validation process took place. The same procedure used to perform the calibration was repeated for the validation. Data was collected from VISSIM using the vehicle record tool and the data was processed using the same Matlab program shown in Figure 23. This time, however, instead of only one simulation being run for each traffic peak, ten runs were performed, each with a different seed number. According to the VISSIM manual [13], the seed number determines the "stochastic variation of input flow arrival times". In other words, it alters the profile of vehicles entering the network. The ten runs were performed for the validation was to ensure that an adequate number of data points were collected. The different seed numbers were not used to ensure randomness of the data. This was a function of the Matlab program which selected vehicles from the vehicle network data in such a way that the data points collected were randomly generated. Each individual run produced its own vehicle record data file to be processed by Matlab. As a result, 1000 data points were obtained representing the simulation. However, upon review of the data, some of the data points were either unrealistic or unusable. Data points that were unusable were those that represented vehicles that did not move during the two minute period. This resulted in a "division by zero" error in the two-fluid model calculations so those points were omitted from consideration.

Unrealistic data points arose from a problem inherent in the two-minute method of data collection. Recall that the two-minute method was imitated for the VISSIM data collection and takes the total distance traveled during a two minute period and extrapolates what would be the travel time for one mile. One of the difficulties with this method is that if a vehicle only travels a few feet due to congestion, the extrapolation results in a travel time of several hours which was not observed in the field. Instead, the accuracy of the distance measurement during field data collection was limited to 0.1 miles, a 20 minute travel time per mile, due the accuracy of the chase car's trip odometer. To account for the loss of accuracy at higher travel times, all data points with a one mile travel time of greater than 20 minutes were omitted from the two-fluid model calculation. However, upon further review of the field data, trip times of greater than ten minutes per mile were rarely encountered, if at all. Since the trip times greater than ten minutes per mile were not represented in the field data, the VISSIM model could not represent them either. Therefore, trips with travel times over ten minutes were also removed from the VISSIM data. This implementation of a heuristic limitation on travel times was also used by Jha et al. [10] where a boundary was placed on travel times from the simulation results so the results would match the field observations. The result of this was the statistical difference between the VISSIM data and the field data shrank considerably. Table 9 and Table 10 show the results of the statistical comparison of the AM and PM peaks, respectively, which was performed as with the calibration. Also, Figure 29 and Figure 30 below show a graphical comparison of the VISSIM and field two-fluid models for the AM and PM peaks. The graphical comparison shows that even though the two lines do not overlap exactly, the models could still be statistically similar. This is because the graph does not show the variation within the data which is best represented in Figure 4 and Figure 6 from Chapter 3.

What the reduction in the statistical difference indicates is that the model calibration performed has an effective accuracy for travel times up to ten minutes. The accuracy of the two-fluid model can be improved by using the field data collected with the one-mile method to perform the calibration. Also, the VISSIM data collection process would have to be modified to select vehicles that have traveled a distance of at least a mile during the data collection window. Such adjustments can be made in the future.

Table 9: Statistical Comparison for AM Peak Validation

		Regression Term A				
	n	ybar	s	SE	t-test	p-value
VISSIM	706	0.327625	0.275278	0.027528	0.175363	0.861202
Field	87	0.343170	0.785934	0.084261		
		Regression Term B				
	n	ybar	s	SE	t-test	p-value
VISSIM	706	0.482374	0.168736	0.016874	0.792423	0.430270
Field	87	0.440450	0.467703	0.050143		

where: n = sample size
ybar = sample mean
s = sample standard deviation
SE = sample standard error
t-test = probability result of Student's T-test
p-value = significance of the statistical results

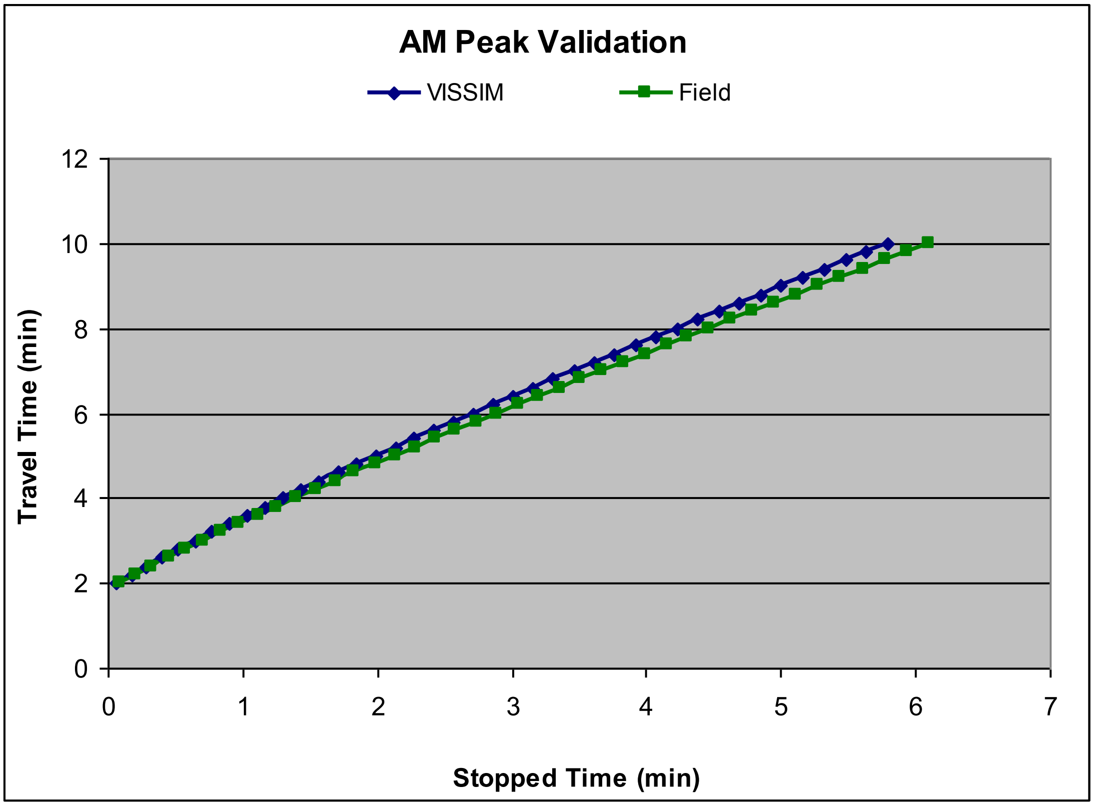

Figure 29: Validated Two-Fluid Model for the AM Peak Network

Table 10: Statistical Comparison for PM Peak Validation

		Regression Term A				
	n	ybar	s	SE	t-test	p-value
VISSIM	585	0.448504	0.590071	0.024396	0.818506	0.415305
Field	87	0.517996	0.758512	0.081321		
		Regression Term B				
	n	ybar	s	SE	t-test	p-value
VISSIM	585	0.412473	0.377354	0.015602	0.679645	0.498534
Field	87	0.377754	0.453721	0.048644		

where: n = sample size
ybar = sample mean
s = sample standard deviation
SE = sample standard error
t-test = probability result of Student's T-test
p-value = significance of the statistical results

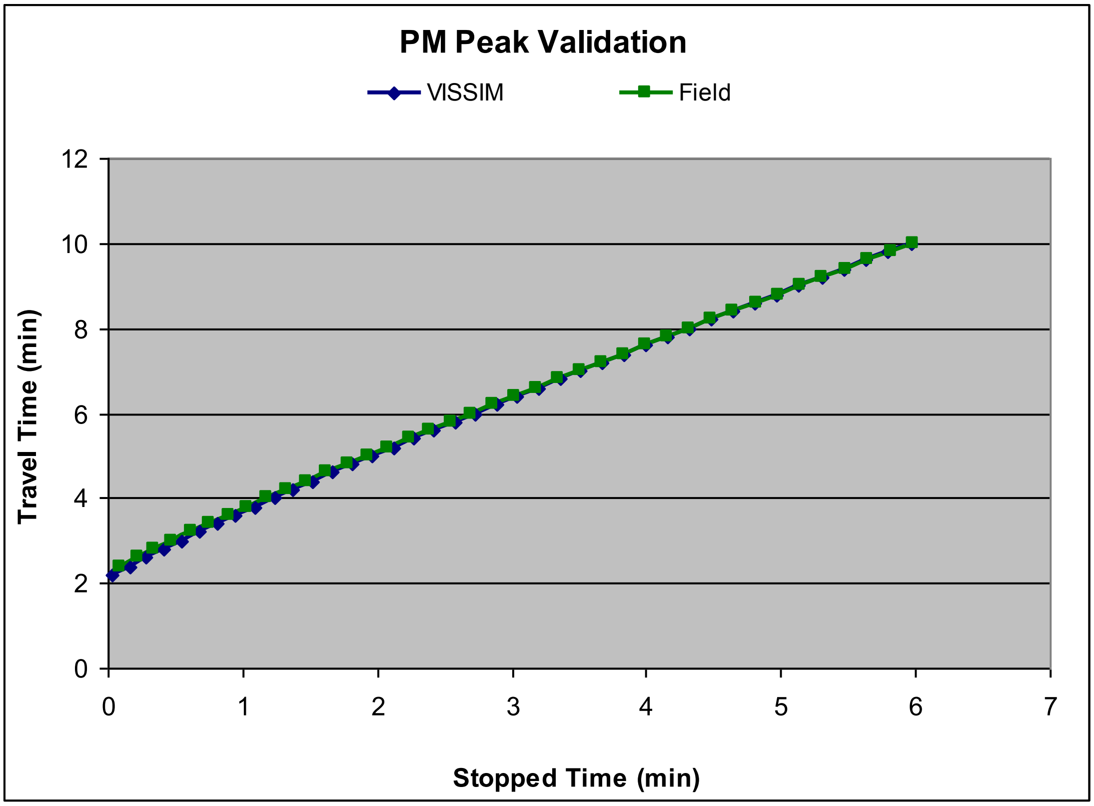

Figure 30: Validated Two-Fluid Model for the PM Peak Network

When analyzing the statistical results for the validation, the goal was to see a p-value of greater than 0.05 or 5% but the higher the value, the more similar the terms were. For the AM peak validation results, regression term A was similar with an 86% confidence and term B was similar with only a 43% confidence. For the PM peak validation results, regression term A was similar with a 42% confidence while term B was similar with a confidence of 49%. Both terms for both peaks were much greater than the 5% cutoff which leads to the conclusion that the calibration of the AM and PM peak in VISSIM was validated. With calibration and validation of the VISSIM model complete, scenario comparison could be performed using the VISSIM model.

CHAPTER 6: SCENARIO COMPARISONS

6.1: Scenario Descriptions

With the VISSIM network calibrated and validated, it was then possible to use it for the purpose of comparing how certain changes might affect the network performance. These scenarios were requested by the city and can be split into two distinct groups described below: base case scenarios and contingency scenarios.

6.1.1: Base Case Scenarios

There were a total of four base case scenarios created for simulation purposes which were the 2008 AM, 2008 PM, 2015 AM, and 2015 PM base cases. All of these scenarios contained unique volumes and signal timings and the 2015 scenarios contained some geometric differences from the 2008 scenarios. It is important to note that the changes made to the original 2008 AM and PM VISSIM network before the validation took place were the networks used as the 2008 base cases. These networks matched the conditions experienced during the November data collection which was decided to be a better suited model to use as a base case because it reflected the completion of construction within downtown. Figure 31 shows the overall 2008 network.

Figure 31: 2008 Base Case Final Network

The 2015 network incorporated a wish list from the city which included projected changes to the network which may or may not happen by the year 2015. The most drastic of these changes was the conversion of the I-4 interchange at Colonial Dr. from a partial cloverleaf to a single point interchange. There were also some lane additions on South St. and Anderson St. between Division Ave. and Rosalind Ave. Figure 32 shows the entire 2015 network. The 2015 network also incorporated greater traffic volumes and different turning movement ratios obtained from the 2015 Synchro file for the PM peak and the 2020 printout for the AM peak.

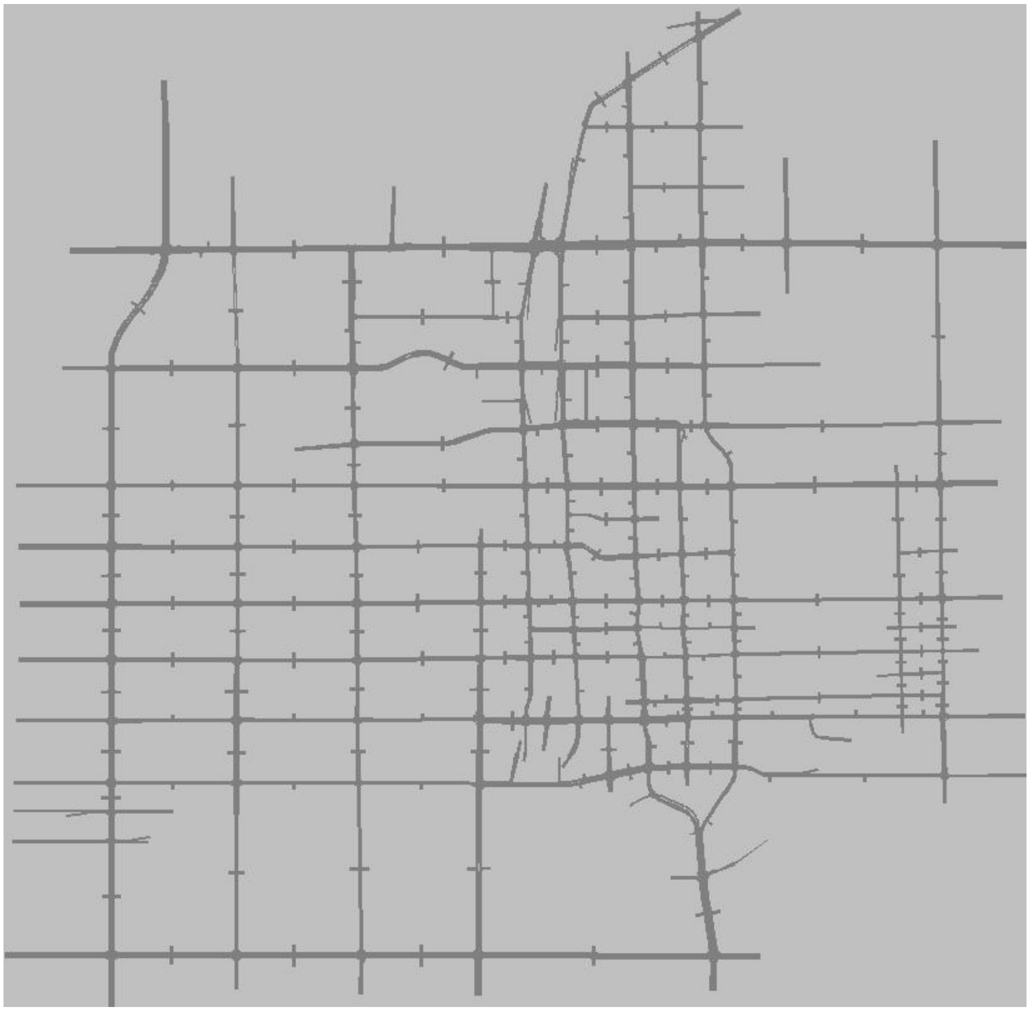

Figure 32: 2015 Base Case Final Network

The comparison outcomes between the base cases were two fold. The effects of both the network changes and new signal timings and offsets would be jointly reflected in the two-fluid model. Even though there was an increase in volumes from 2008 to 2015, this would not necessarily affect the two-fluid model because heavier traffic simply provides a larger number of points with higher travel times per mile which are, in theory, part of the same model that would be generated if the traffic was extremely light.

6.1.2: Contingency Scenarios

The primary distinction between the contingency scenarios and the base case scenarios is that the contingencies were all derived from one of the four base cases. This meant that there were no changes to signal timings or traffic volumes in the network as a whole. The only changes made between the base case and the contingency were simulation elements required to create the desired effect. In some instances, this did require adding volume or installing new signals, but, for the most part, the networks remained unchanged. There were four different contingencies the city requested. Three required an AM and PM VISSIM model to be created and one only required the PM model resulting in a total of seven scenarios modeled in VISSIM.

The first contingency, modeled as Scenario 1 and 2, was to test the effect of an incident such as construction or an accident resulting in the closure of one lane on a critical link used for the given peak. The critical link selected was different for each peak. For the AM peak, the left lane on South St. between Rosalind Ave. and Magnolia Ave. was closed at the midblock location as shown in Figure 33. The closure was positioned such that vehicles would still be able to turn at downstream locations and would still be able to use the midblock driveways. The closure location for the PM peak was located on the left lane of Orange Ave. between Church St. and Jackson St. as shown in Figure 34.

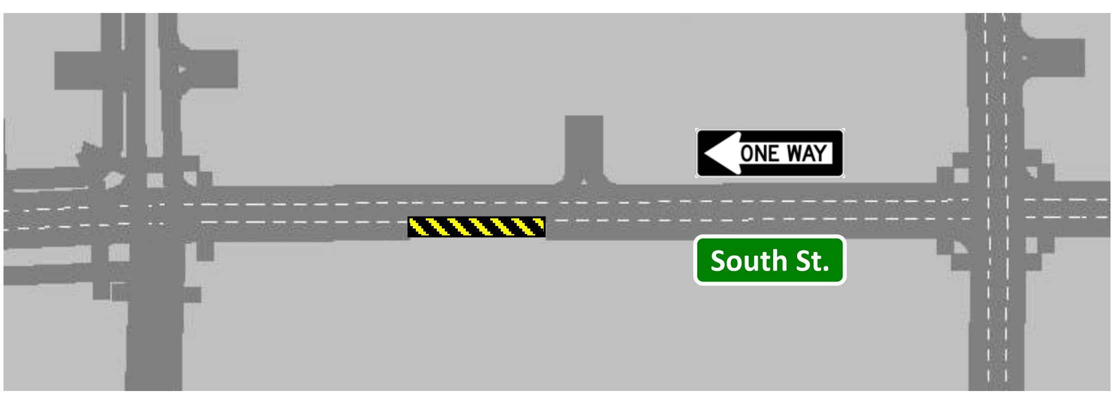

Figure 33: Scenario 1 – Left Lane Closure on South St.

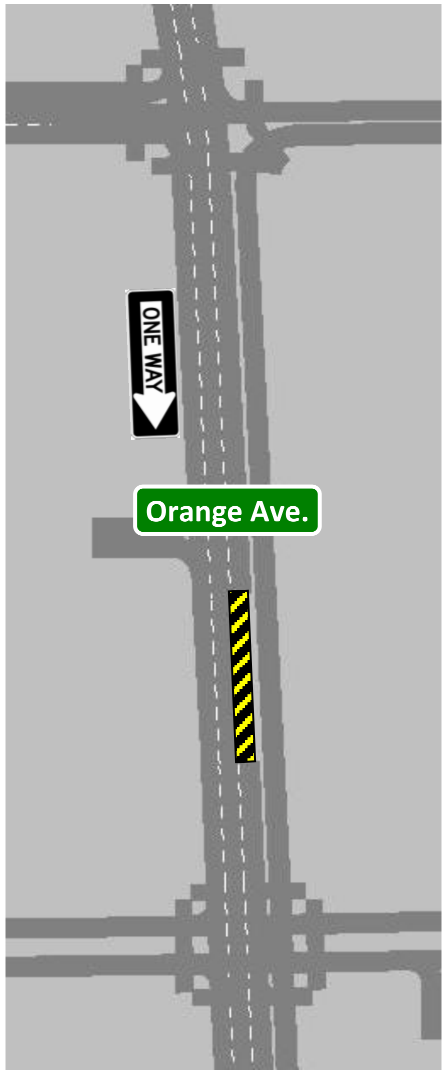

Figure 34: Scenario 2 – Left Lane Closure on Orange Ave.

The second contingency, Scenario 3, was to see the effects of overlapping the normal PM peak traffic with the traffic expected to be traveling to the new Orlando Downtown Events Center. This was probably the most complex scenario to model because it called for the closure of two roadway segments, the rerouting of the traffic affected by the closure, distribution of the extra volumes from 14 different origins to 11 destinations, and insertion of small geometric elements meant the simulate realistic turning movements of arriving vehicles. The two road segments that were closed for the scenario were Division Ave. between Church St. and South St. and Church St. between Hughey Ave. and Division Ave. This closure is shown in Figure 35.

Since the intersection of Division Ave. and Church St. effectively became a two leg intersection, the signal was rendered invisible to the simulated vehicles. All traffic that was to be using a closed roadway segment was sent on one of the detours listed below.

- NB Division Ave.: W on South St. - N on Parramore Ave. - E on Church St. - N on Division Ave.
- SB Division Ave.: W on Church St. - S on Parramore Ave. - E on Anderson St. - S on Division Ave.
- EB Church St.: N on Division Ave. - E on Central Blvd. - S on Hughey Ave. - E on Church St.
- WB Church St.: S on Hughey Ave. - W on South St. - N on Parramore Ave. - W on Church St.

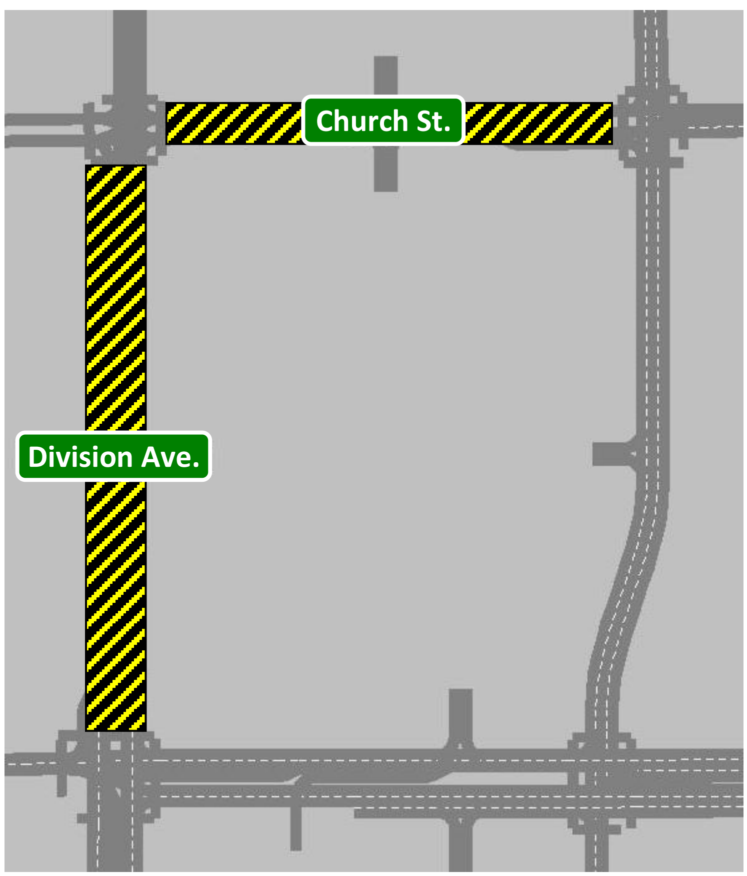

Figure 35: Scenario 3 – Closure of Division Ave. and Church St.

As for adding the extra volume traveling to the events center, Figure 36 provided by the city shows the amount of extra traffic expected on streets around the center heading for surrounding parking garages. Figure 36 also shows the number of vehicles coming from network entrances and the number that each garage or lot is expected to hold. To simplify entering this data into VISSIM, an origin-destination matrix, shown in Table 11, was created by assigning each traffic source a letter and each destination a number. Then using simple arithmetic, the number of vehicles traveling from each origin to each destination was calculated. There was some assumption involved in determining where the origins traced back to. For example, for the extra volume on Anderson St., it was assumed that the volume first entered the network traveling northbound on OBT and then turned onto Anderson. The assumed project area origins are all stated in Table 11. It was stated above that along with the road closures, minor geometric changes were done to better simulate the parking entrances. This was mostly done by adding a second driveway on the other side of a one-way street or by inserting a median turn lane where none had existed before. With the origin, path, and destination set for the extra volumes, all that remained was to enter them into VISSIM. This was done using the procedure below.

- Increase the vehicle input volumes at the affected VISSIM network entrances.
- Select the routing decision for each of the affected entrances and create an exclusive route from the network entrance to all the parking destinations used by that entrance.
- Using the origin-destination matrix, assign the appropriate amount of volume to each of the new routes.

Because this contingency simulated conditions of an evening event, there was no need for an AM peak model to be made which meant that Scenario 3 was ready for simulations.

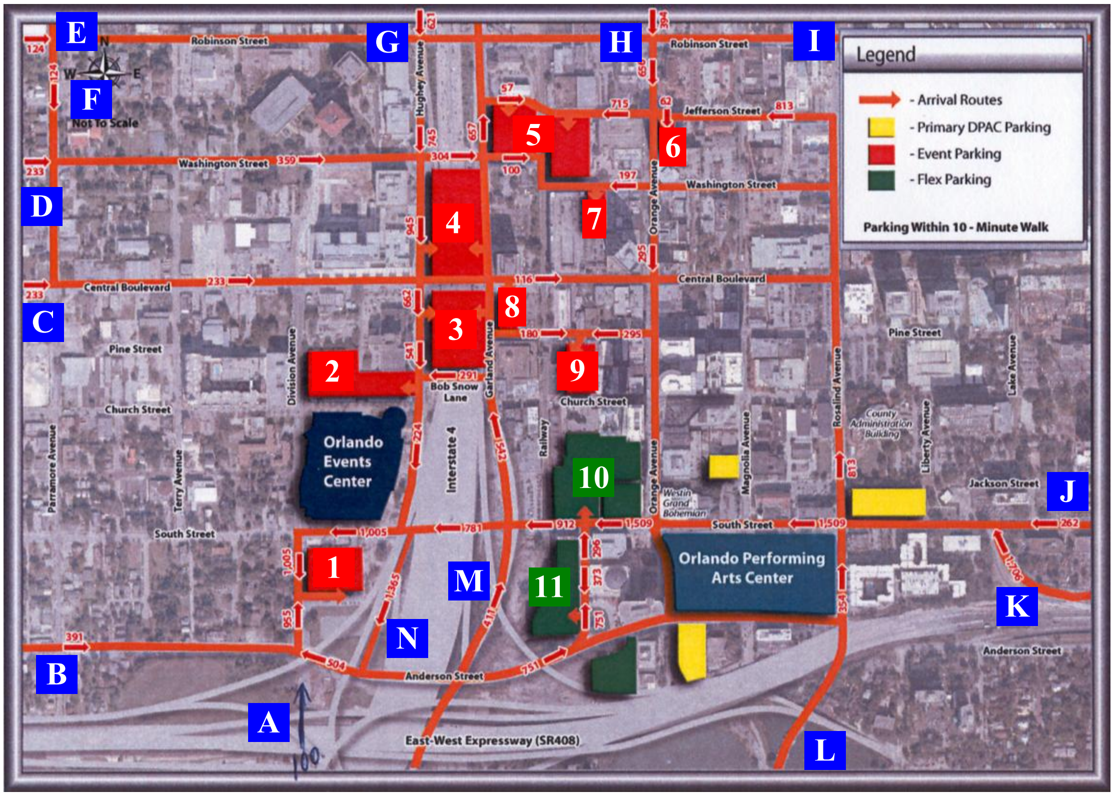

Figure 36: Scenario 3 - Extra PM Peak Volumes due to Events Center Traffic

Table 11: Scenario 3 Origin-Destination Matrix

Origins (Network Entrance)	Destinations											
	1	2	3	4	5	6	7	8	9	10	11	SUM
A (NB Division Ave.)	60											60
B (NB OBT)	391											391
C (EB Central Blvd.)		117						116				233
D (EB Washington St.)				200	33							233
E (SB OBT)				124								124
F (EB Colonial Dr.)					24		100					124
G.1 (WB I-4 @ Colonial)		200	121									321
G.2 (WB Colonial Dr.)	224			76								300
H (SB Orange Ave.)							99		295			394
I (WB Robinson St.)							62					62
J (WB South St.)											262	262
K (WB SR-408)	781	131			459					224	111	1706
L (NB Orange Ave.)					256	62	36					354
M (EB I-4)		160	116						180			456
N (WB I-4 @ Anderson)	504									296	455	1255
SUM	1960	608	237	400	772	62	297	116	475	520	828	6275

The third contingency involved the expansion of the Lymmo Bus Rapid Transit service that already exists on the network. This contingency, which became Scenarios 4 and 5, dictated that one bus lane be added to Orange Ave. and Magnolia Ave. between Amelia St. and where Orange Ave. turns to the northeast. The bus lanes were modeled to be contraflow lanes which meant that the buses traveled in the opposite direction of the traffic on the one-way streets where they were located. The addition of the contraflow lane to Magnolia Ave. did not affect the three existing general use lanes although some of the intersections had to be resized. However, since the affected portion of Orange Ave. had four general use lanes the city wanted to see the effects of occupying one of those lanes to make room for the contraflow lane. This reduced the general use lanes to three between Garland Ave. and Amelia St. Figure 37 shows the new contraflow lanes and their intersections with Colonial Dr.

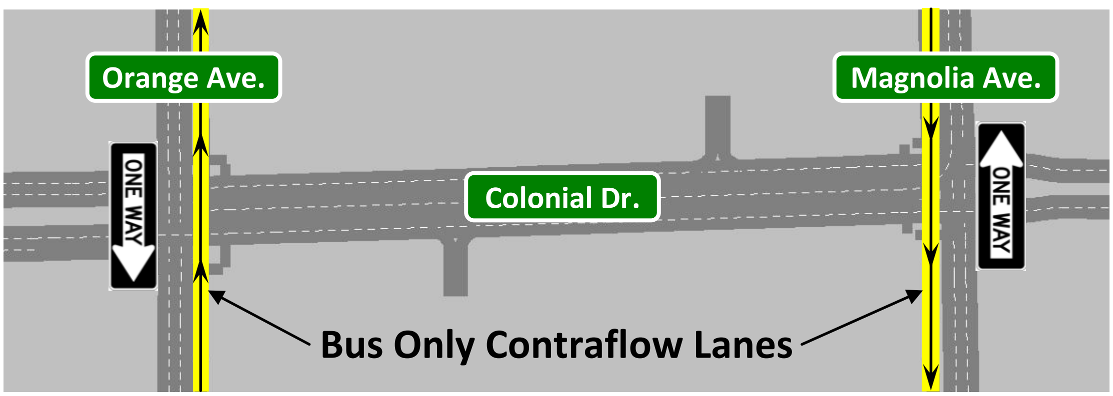

Figure 37: Scenarios 4 & 5 – Contraflow Lanes for Northern Lymmo Route

At either end of the new contraflow lanes, it was assumed that the buses would enter the normal traffic pattern. Since the transit expansion was meant to include a new Lymmo line with greater range, the pre-existing Lymmo route was retained and a new one was set to run on the new lanes. This new route, picture as the yellow line in Figure 38, traveled down the new lanes, went through the simulated Lynx Transit Center, and then ran a circuit of the original Lymmo lanes before returning on the new contraflow lane. This contingency applied to both the AM and PM peaks so a VISSIM model was created for each.

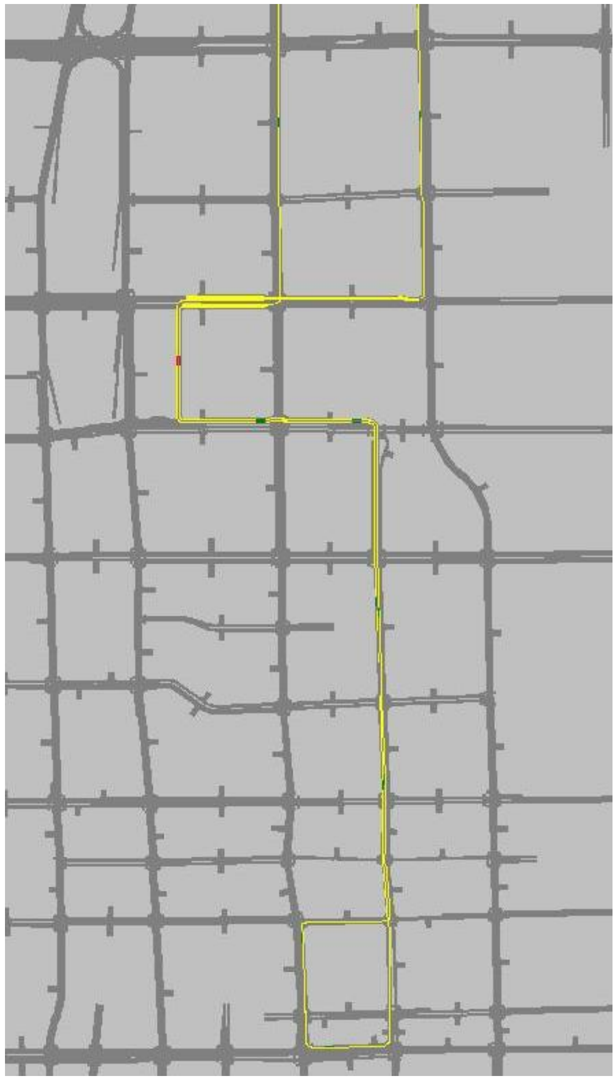

Figure 38: New Lymmo Route on New and Original BRT Lanes

The fourth and final contingency, which was named Scenarios 6 and 7, involved the addition of a completely new north-south, signalized corridor called Terry Ave. to the western half of the network. At present, Terry Ave. is a two lane local roadway which runs from Anderson St. to Robinson St. It only has two signalized intersections at Church St. and Central Blvd. which were not included in the original base case networks. The reason the city asked for a contingency including Terry Ave. is because there are plans to extend Terry Ave. to the north across Livingston St., Amelia St., and Concord St. to then align with Edgewater Dr. at the Colonial Dr. intersection. Terry Ave. would become Edgewater Dr. after crossing Colonial Dr. To the south, it is possible that the city might extend Terry Ave. underneath SR-408 down to Gore St. but this was not included in the model. Though it may seem like this would be the most complex contingency to enter into VISSIM, it was very similar to modeling Westmoreland Dr. from scratch when no Synchro import was available. The "proofing" procedure use when modeling the calibration and base case networks was followed to model Terry Ave. The city had provided information about assumptions that could be made about Terry Ave. which were:

- The cross section would be a two-lane, two-way roadway placed halfway between Division Ave. and Parramore Ave.
- The volumes on Terry Ave. would be the same as Parramore Ave. from Anderson St. to Livingston St. and half of Parramore Ave. from Livingston St. to Colonial Dr.
- All intersections would be signalized except the ones at Anderson St., Livingston St., and Concord St. which would be stop controlled.
- There would be left turn lanes as needed. The criterion used for left turn lanes was that the intersections with the same volumes as Parramore Ave. had turn lanes and the rest did not.

Other assumptions had to be made. For instance, the timings and offsets for the new signals were assumed to be the same as Parramore Ave. as well as the turning movements for the Terry Ave. intersections. Also, for the stop controlled intersections, it was assumed that two-way stop control would be used and, in all cases, Terry Ave. traffic would have to stop. Figure 39 shows the network with the complete addition of Terry Ave.

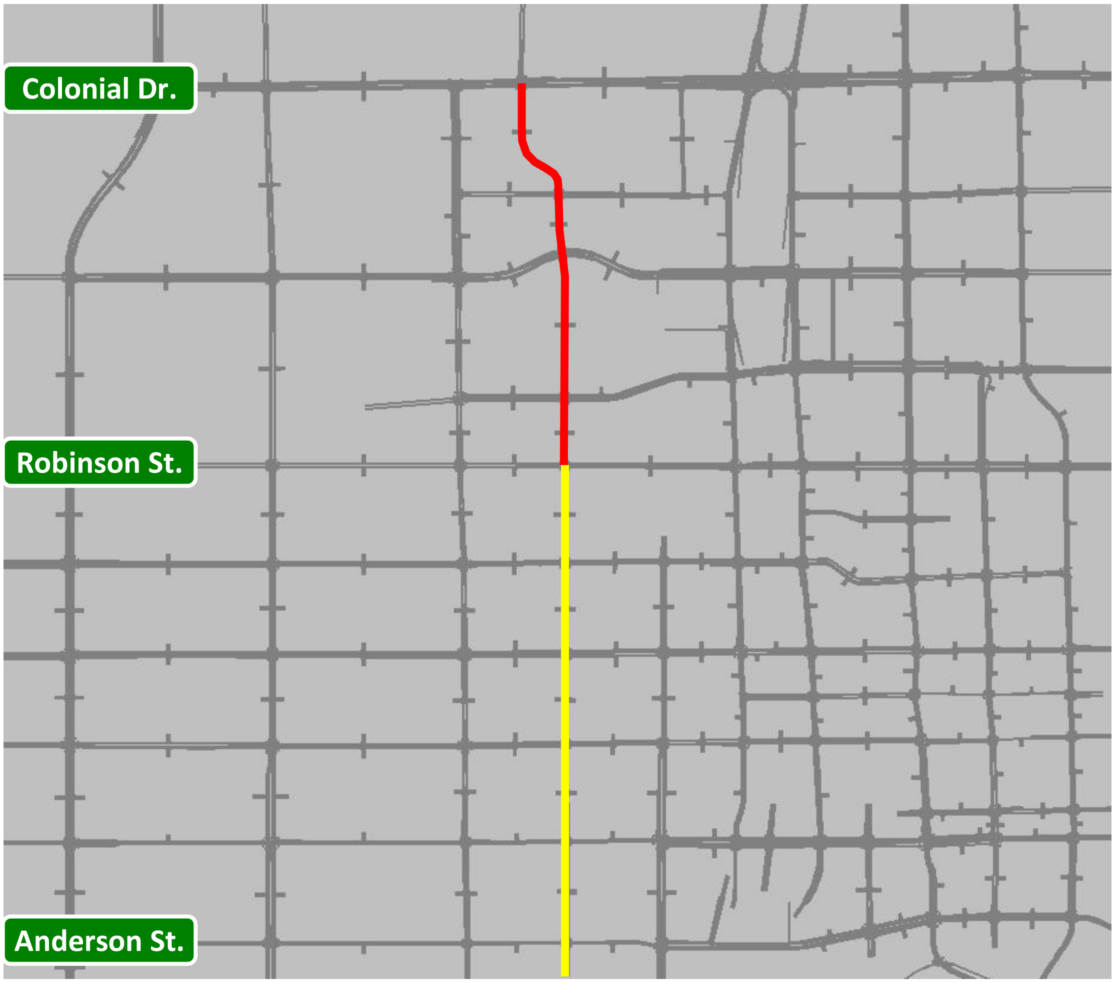

Figure 39: Scenarios 6 & 7 – Terry Ave. (yellow) with Proposed Extension (red)

6.2: Comparison of Different Years Using the Base Cases

As stated previously, the two-fluid model can be used to reflect both temporal and geometric differences between two VISSIM models. For this project, the 2008 base case was compared to the 2015 base case with the same traffic peak. The procedure used to generate the two-fluid model for the calibration and validation was employed for the comparisons in the section. Figure 40 and Figure 41 show the graphical representation of the two-fluid models for the base cases and Table 12 lists the two-fluid model parameters along with a statistical significance comparison of the two terms used to generate the two-fluid model parameters.

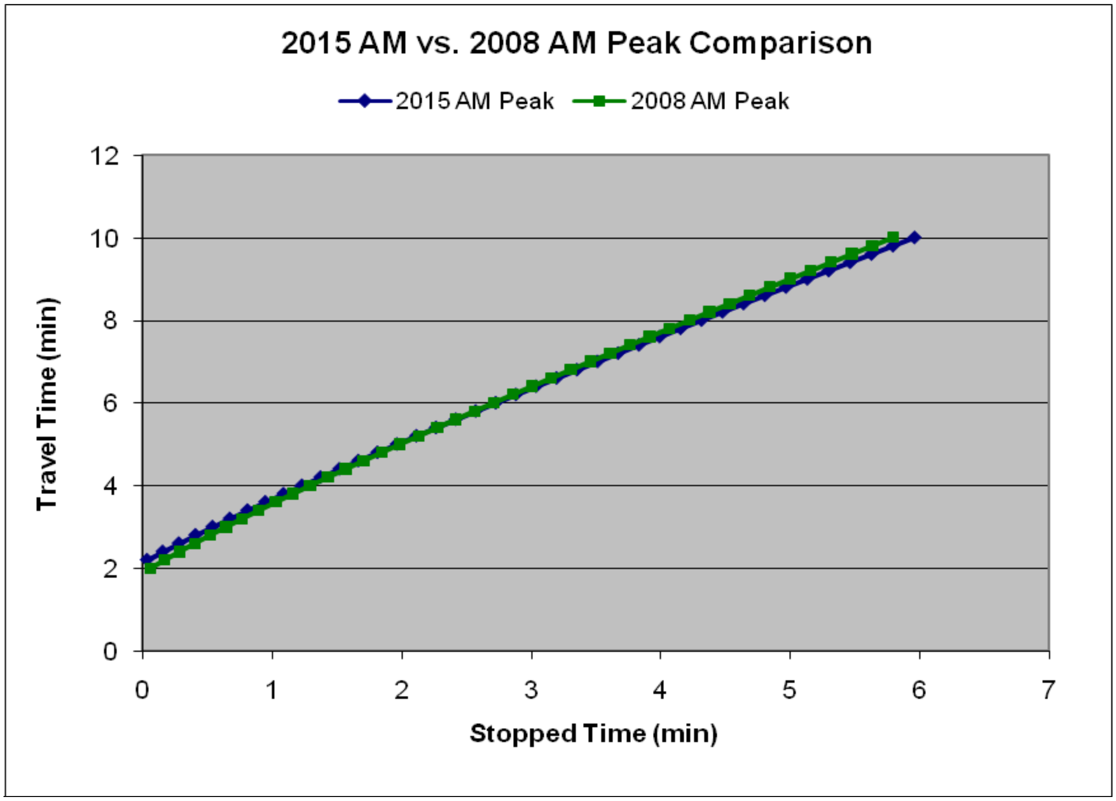

Figure 40: 2008 AM vs. 2015 AM Base Case Two-Fluid Model Comparison

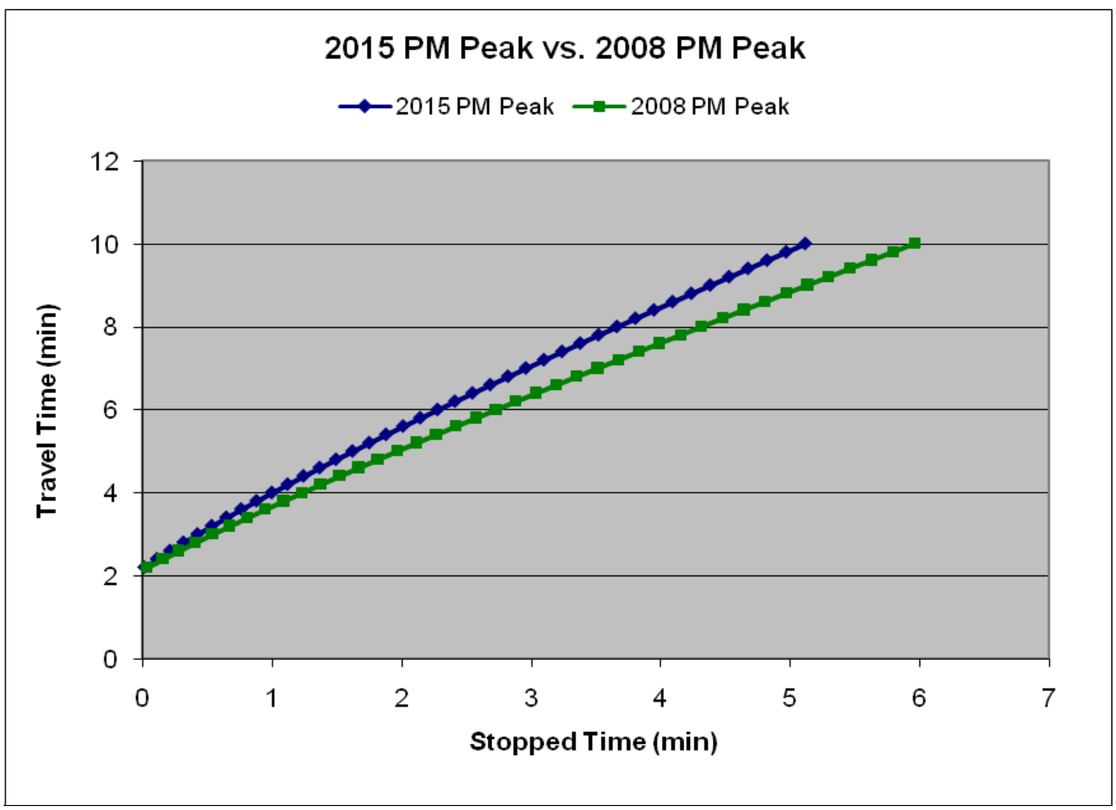

Figure 41: 2008 PM vs. 2015 PM Base Case Two-Fluid Model Comparison

Table 12: Base Case Statistic and Parameter Comparison

Scenario Names	Statistical Comparison		Two-fluid Parameters	
	A (p-value)	B (p-value)	T_m	n
2008 AM Peak	0.009111	0.012881	1.88	0.93
2015 AM Peak			2.14	0.70
2008 PM Peak	0.036836	0.000006	2.14	0.70
2015 PM Peak			2.17	1.13

From the p-values in Table 12 it is clear that the performance of both 2008 peaks were statistically different from the performance of the 2015 peak. With the statistical comparison, when the p-value is less than or equal to 0.05, the differences between the two base cases or scenarios can be considered statistically significant. If the p-value is greater than 0.05, the two scenarios cannot be considered to have statistically significant differences. This is the same means of comparison used to calibrate and validate the VISSIM model. Upon visual inspection of the two-fluid graphs, the curious finding is that the 2015 AM network performed better under congestion than the 2008 AM network while the reverse was true for the PM networks. The two PM networks perform about the same near free flow conditions but the 2015 network performance worsens more rapidly than the 2008. The worse performance of the 2015 PM network could be caused by the different signal timings used in that network which could not handle the larger volumes effectively. The two-fluid model doesn't indicate directly what caused the worse performance. However, what is known is that the 2015 PM network handled the larger volumes worse than the 2008 network handled smaller volumes.

6.3: Comparison of Contingencies with Corresponding Base Cases

The same comparison technique performed on the four base case scenarios was also carried out on the seven contingency scenarios. These comparisons were different from the base case comparisons because all of the contingencies were compared with the base case from the same year and traffic peak. This limited the factors that could affect the two-fluid model to alterations that were made to create the contingency specified. Figure 42 to Figure 48 below show the graphical comparisons of the contingency two-fluid models with their base case two-fluid models and Table 13 to Table 16 list the two-fluid model parameters and the statistical significance between the similarities of the terms used to generate the model parameters.

Figure 42: Scenario 1 vs. Base Case Two-Fluid Model Comparison

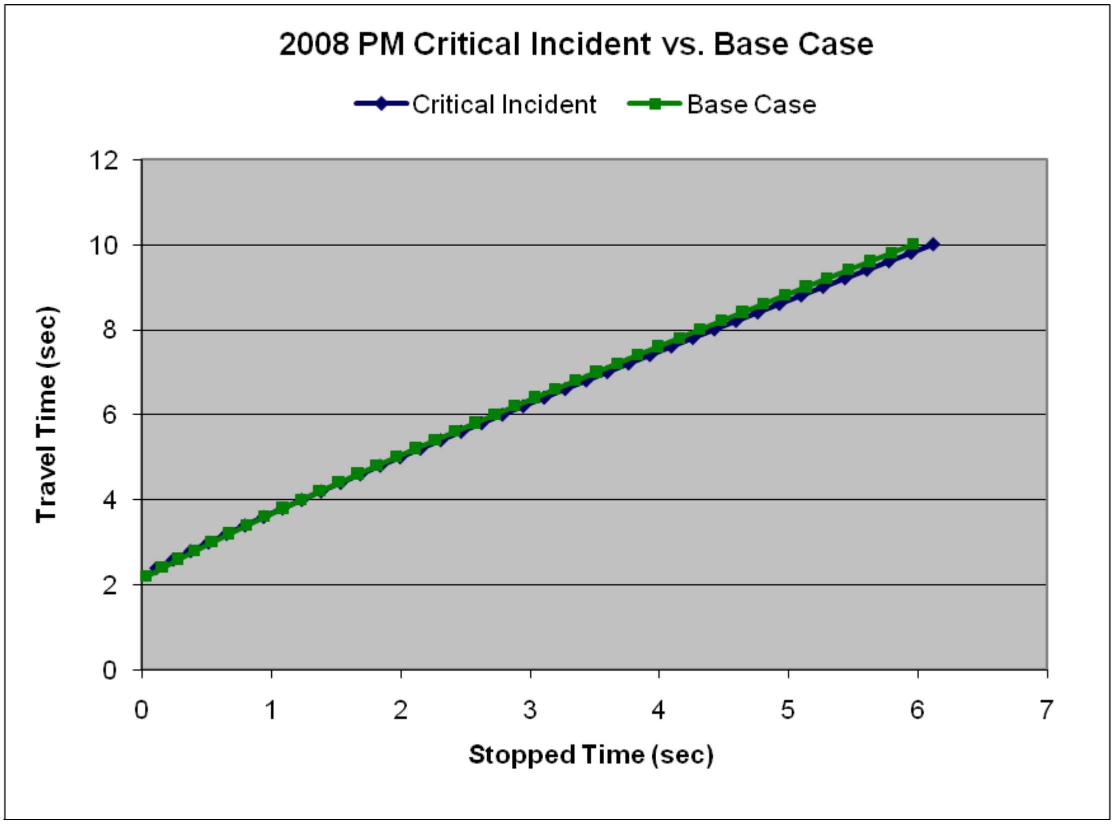

Figure 43: Scenario 2 vs. Base Case Two-Fluid Model Comparison

Table 13: Scenarios 1 & 2 Statistic and Parameter Comparison

Scenario Names	Statistical Comparison		Two-fluid Parameters	
	A (p-value)	B (p-value)	T_m	n
2008 AM Incident	0.087910	0.054752	1.42	1.57
2008 AM Base Case			1.88	0.93
2008 PM Incident	0.147692	0.093721	2.22	0.59
2008 PM Base Case			2.14	0.70

According to the statistics, neither of these scenarios produced a statistically significant difference from the base case. However, both of the AM peak values and one PM peak value were somewhat significant since they were close to a p-value of 0.05. Upon review of the graphs, the AM incident did have a more considerable change to the two-fluid model than the PM incident. This may have been because the lane reduction occurred on a link many vehicles used before spreading to the downtown network. Therefore, the reduction from three to two lanes produced a metering effect on the rest of the network downstream by limiting the throughput and preventing congestion. Even though the closure produced a backup on the affected roadway, it was somewhat isolated since the queue traced back to two major network entrances where the congestion “left the network”. For the PM incedent the same metering effect occurred. However, more of the queue that formed remained on the network thereby affecting network performance reflected in the two-fluid model.

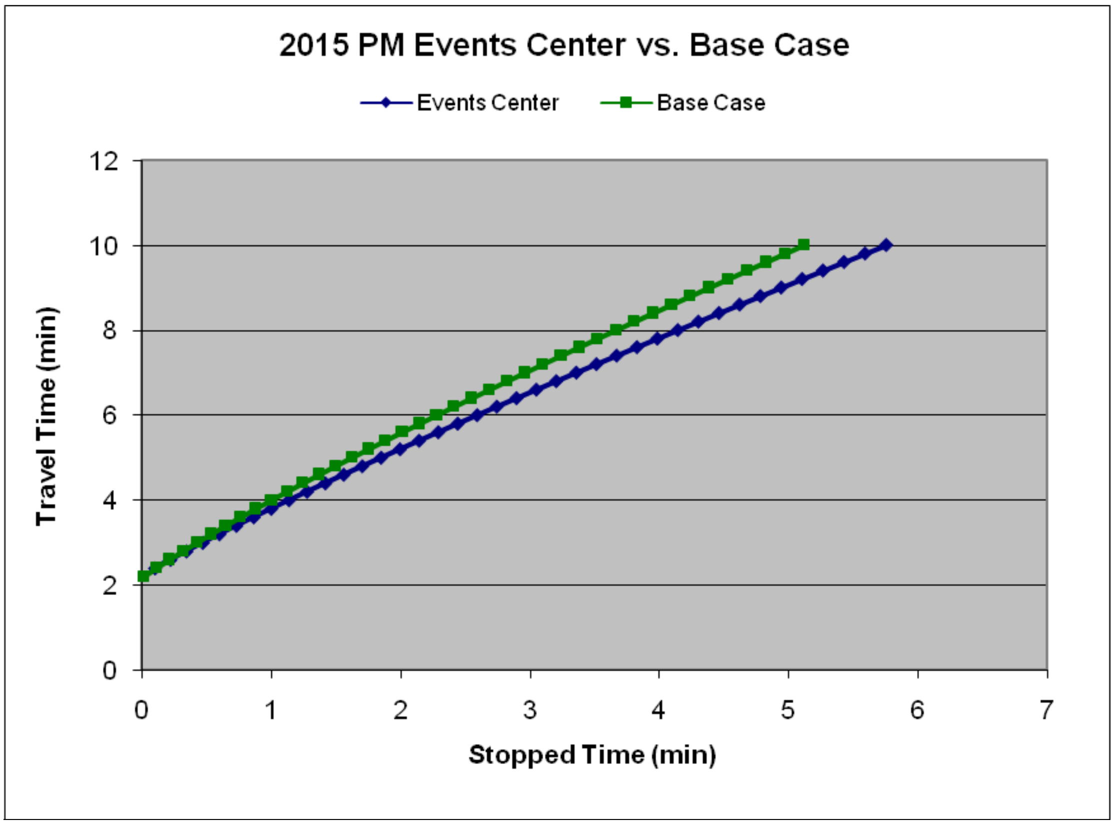

Figure 44: Scenario 3 vs. Base Case Two-Fluid Model Comparison

Table 14: Scenario 3 Statistic and Parameter Comparison

	Statistical Comparison		Two-fluid Parameters	
Scenario Names	A (p-value)	B (p-value)	T_m	n
2008 PM Events Center	0.031310	0.000378	2.23	0.75
2008 PM Base Case			2.17	1.13

The results of the events center comparison at first don't seem to make much sense. Two road segments are closed and a large number of extra vehicles are placed on the network and yet the performance improves according to the two-fluid model. Even the statistics state that the two networks are significantly different according to the p-values in Table 14. To respond to this confusion, it is first important to remember that just because the volume on a network increases does not mean that the performance will worsen. So why does the performance improve? In the case of the events center, the only volumes of the network that were increased were those on certain links carrying vehicles heading to parking garages. Another look at Figure 36 reveals that most of the extra traffic was traveling in the opposite direction of the PM peak traffic and, in some cases, using roads that were normally underutilized. This would be expected since the events center traffic was trying to enter the network and the PM traffic wished to exit. What may have resulted was that the number of vehicles on less used roads in the network increased, improving the average, or macroscopic performance of the network.

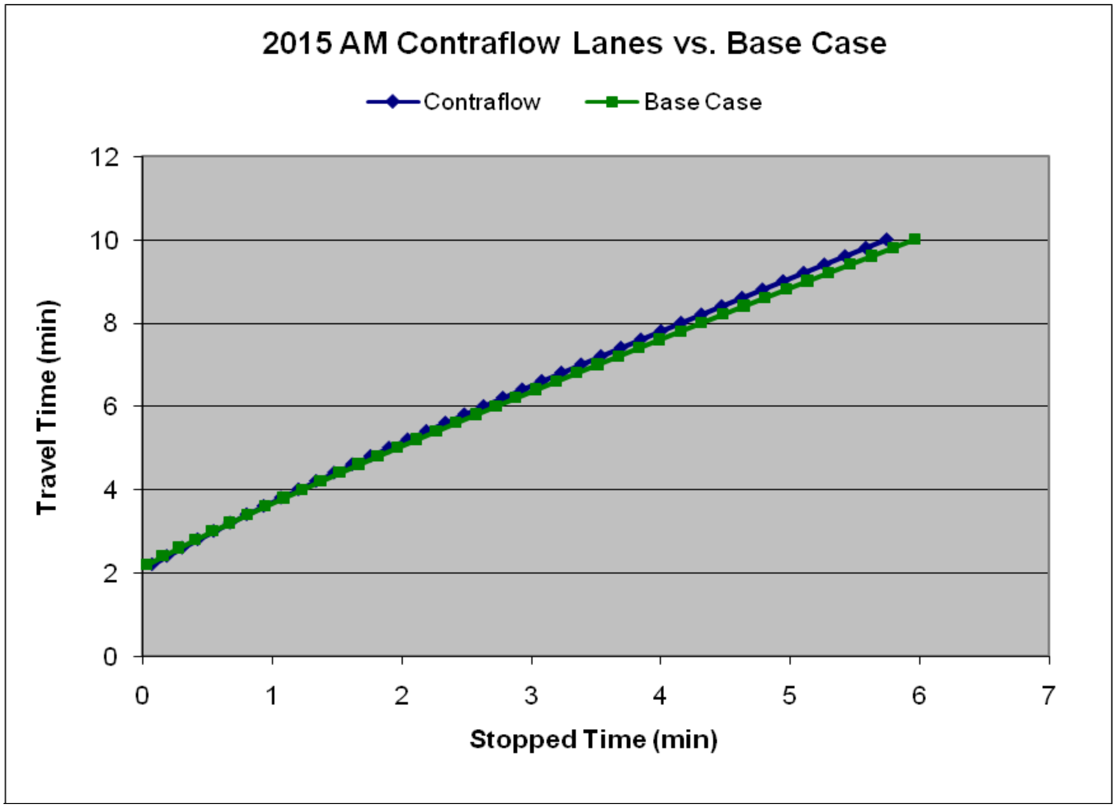

Figure 45: Scenario 4 vs. Base Case Two-Fluid Model Comparison

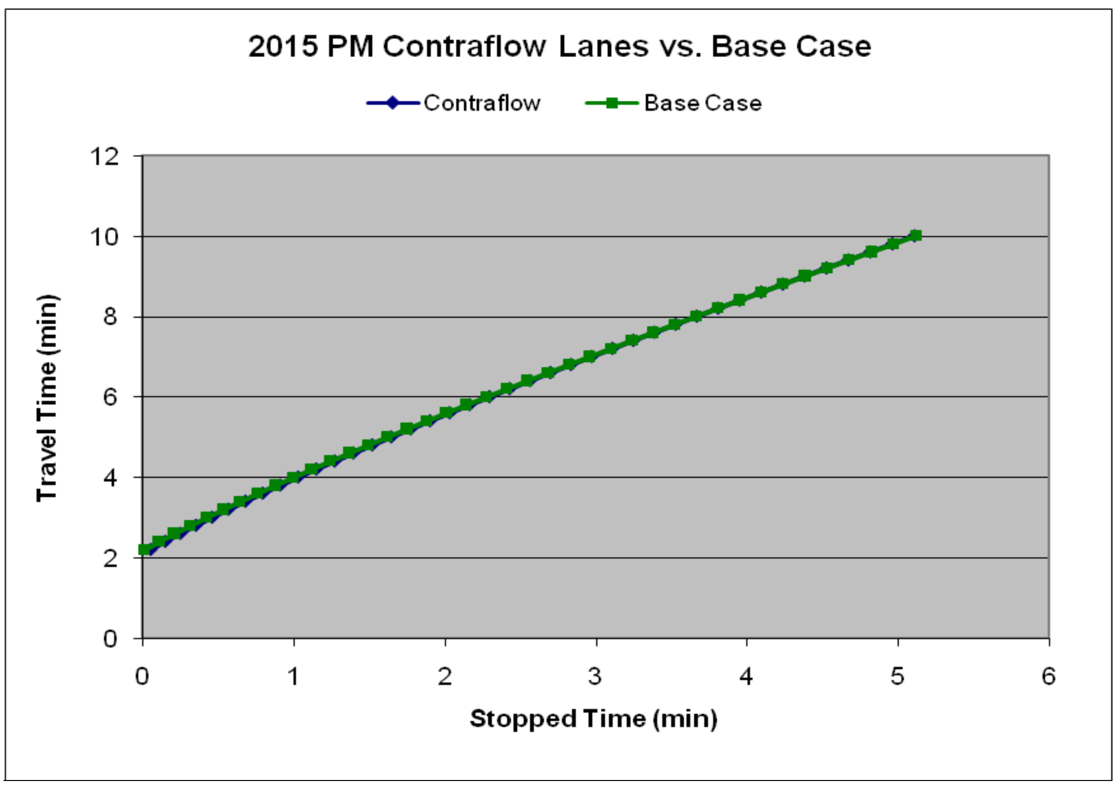

Figure 46: Scenario 5 vs. Base Case Two-Fluid Model Comparison

Table 15: Scenarios 4 & 5 Statistic and Parameter Comparison

Scenario Names	Statistical Comparison		Two-fluid Parameters	
	A (p-value)	B (p-value)	T_m	n
2015 AM Contraflow	0.283793	0.146313	2.06	0.85
2015 AM Base Case			2.14	0.70
2015 PM Contraflow	0.552246	0.538565	2.09	1.19
2015 PM Base Case			2.17	1.13

As is clear in the statistics and in the graphs, there was very little significant difference in the network performance due to the addition of the contraflow bus lanes. According to the graph of the AM peak comparison, the ability of the network to handle congestion does decrease slightly due to the contraflow lane. However, this is most likely the results of the northern blocks of Orange Ave., a heavily used section during the AM peak, being narrowed from four lanes to three. This also explains why the performance reduction is practically non-existent in the PM peak since the affected segment of Orange Ave. is not heavily traveled during that peak.

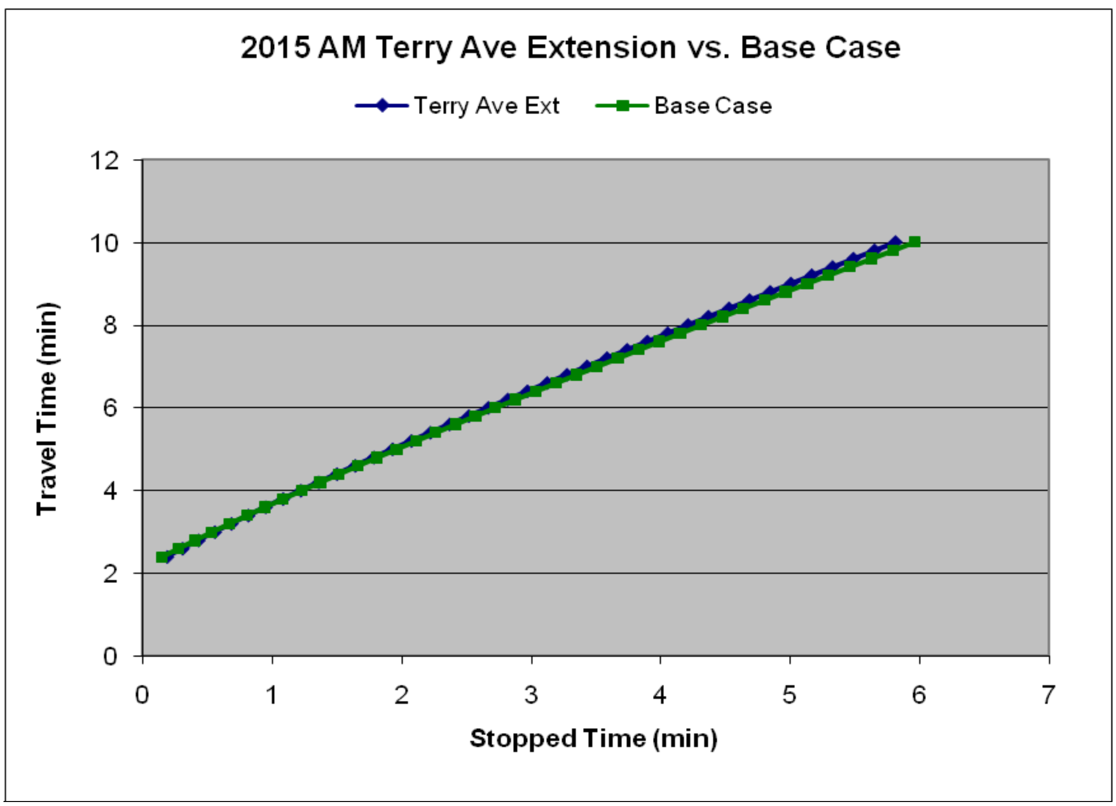

Figure 47: Scenario 6 vs. Base Case Two-Fluid Model Comparison

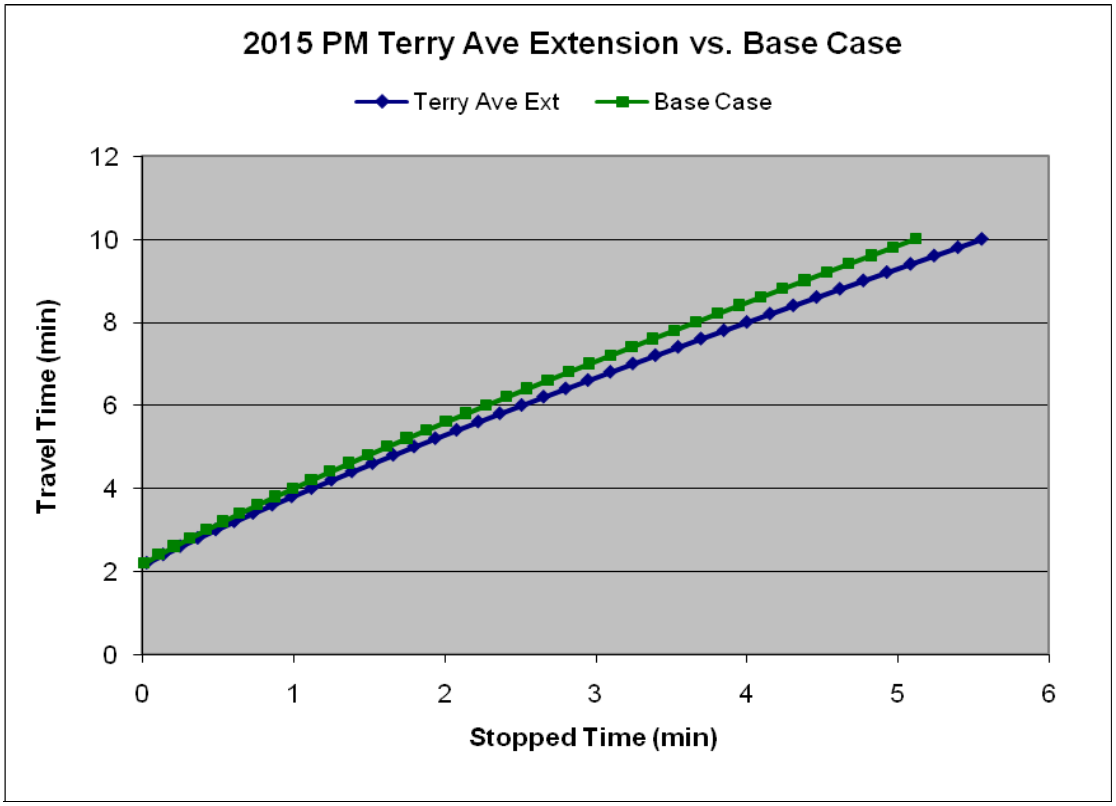

Figure 48: Scenario 7 vs. Base Case Two-Fluid Model Comparison

Table 16: Scenarios 6 & 7 Statistic and Parameter Comparison

Scenario Names	Statistical Comparison A (p-value)	Statistical Comparison B (p-value)	Two-fluid Parameters T_m	Two-fluid Parameters n
2015 AM Terry Ave.	0.396282	0.252536	2.07	0.81
2015 AM Base Case			2.14	0.70
2015 PM Terry Ave.	0.424013	0.052748	2.14	0.90
2015 PM Base Case			2.17	1.13

For the Terry Ave. extension contingency comparison, there was not a statistically significant difference between the results even though B for the PM peak was somewhat significant. According to Equation 5, *n* is calculated using B which coincides with the Terry Ave. PM graph having such a different slope from the base case. A further look at the graphs also reveals a distinct difference between the AM peak and PM peak comparison. For the AM, the network with Terry Ave. responds worse to congestion than the base case while the PM network with Terry Ave. responds better to congestion. There is no reasonable way to explain for sure why this happened except that it is a difference the two-fluid model is sensitive to that is immediately inexplicable. A possible explanation is that for the AM peak, the addition of Terry Ave. acted as an additional barrier for traffic entering downtown from the west to cross, decreasing performance slightly. However, in the PM peak, the addition of Terry Ave. provided an additional means for vehicles exiting the network to leave more directly. Both of these arguments could be made for both traffic peaks but it is possible that for each peak, the effects of one outwighed the effects of the other.

CHAPTER 7: CONCLUSION

According to the research presented in this thesis, the calibration and validation of multiple VISSIM network was a success. In fact, the significance of the final validation is evidenced in the many differences between the February and November networks. Even after so many changes had been made to the network, the calibration of VISSIM maintained its validity which speaks to the success of this technique. The use of the macroscopic models such as the two-fluid model as a calibration tool for microsimulations such as VISSIM is still a new concept but one with great promise. The methods presented in this thesis have shown that microsimulation calibration can be achieved without the complexity or man hours of typical calibration techniques. This quicker calibration approach offers a way for transportation agencies to evaluate the effects of suggested improvement alternatives to their networks before construction takes place. As showcased in this thesis, several suggested improvements to the Orlando, Florida, downtown network were evaluated using the VISSIM simulation calibrated with the two-fluid model. The following paragraphs contain a summary of the network comparison results.

A comparison of the two-fluid models collected from the network in February and November reveals that the changes made to the network improved the ability of the AM and PM peak networks to handle congestion which was shown by lower values for n for those peaks. The midday peak did not experience a significant change to the value of n. On the other hand, the performance of the network under free flow conditions for all traffic peaks worsened from February to November as shown by the higher values for T_m.

As stated previously, the primary application of the calibrated VISSIM simulation is that the effects of proposed changes to the downtown network can be seen prior to construction by making those changes in VISSIM, obtaining the new two-fluid model, and comparing the simulation model with the existing network's model. A comparison was performed between the four base case networks from two different years and two different traffic peaks. In the base case comparisons, the 2008 AM Base Case was compared with the 2015 AM Base Case. The result was that the 2008 AM network performed better in free flow conditions while the 2015 AM network performed better under congested conditions. Also, the 2008 PM Base Case was compared with the 2015 PM Base Case. The results there showed that the networks were similar in free flow conditions but the 2008 PM network handled congestion more effectively.

Along with the base case comparisons, seven different scenarios were modeled and compared with their parent base case. For these comparisons, whatever year and traffic peak the scenario took place in, that base case was the network it was compared with. For the two scenarios set in 2008 with incidents on critical links, the base case performed better in the AM peak but the networks performed almost identically in the PM peak. Also, there was no statistically significant difference in these comparisons. The third scenario involving overlapping traffic heading to the Orlando Events Center onto the normal PM peak traffic in the year 2015 actually showed that the network with the events center traffic performed better than the base case. This may have been because more of the network was being utilized by traffic entering the network and using streets which would normally have been underused. The fourth and fifth scenarios involved placing contraflow bus lanes on the 2015 AM and PM networks. The comparison results were that the AM base case performed slightly better and the PM networks were almost identical. The small difference in the AM peaks was most likely due to the reduction of Orange Ave. from four lanes to three. Still neither of the comparisons produced statistically different results. The sixth and seventh scenarios modeled the effects of the addition of Terry Ave., a new signalized corridor, to the network and its extension to Colonial Dr. in the year 2015. The comparison of the AM peaks showed very little difference, with the base case performing slightly better. However, the PM results showed that the addition of Terry Ave. improved the network performance during congestion. Still, neither of the comparisons was statistically different.

Even though the calibration and validation procedure outlines in this thesis was a success, there is still room for refinement of the concept. The existing two-fluid models lose accuracy as travel time exceeds 20 minutes due to the usage of data collected with the two-minute method. Future work should look into collecting data on the physical and virtual network in such a way that one-mile travel time data could be used. Such data has the potential to produce a more accurate two fluid model which would account for vehicles with travel time greater than 20 minutes. Additional work could also be done to explore the usage of different driving behavior parameters to perform the calibration.

APPENDIX A: FEBRUARY 2008 RAW DATA

AM Peak 1-mile Raw Data

Total Time			Running Time			Number of Stops
min	sec	ms	min	sec	ms	
3	45	87	2	36	53	4
4	4	3	2	54	60	3
4	18	84	3	28	57	5
5	13	63	3	29	85	5
5	1	34	3	24	84	8
4	17	9	2	55	48	3
2	55	94	2	27	50	3
2	45	59	2	8	79	3
3	58	65	2	51	53	3
3	28	50	2	51	88	3
5	36	12	3	11	17	4
6	42	47	4	7	3	6
4	2	12	2	14	28	3
4	58	47	3	17	3	5
3	34	54	2	11	32	3
2	39	3	2	12	19	2
5	40	34	2	56	45	6
6	33	78	3	12	7	7
3	54	75	2	38	79	3
7	52	50	3	57	6	8
5	3	50	3	31	22	4
2	29	50	1	34	8	1
5	41	68	2	29	19	4
6	27	69	3	42	78	4
4	36	12	2	48	68	4
3	42	82	2	11	37	3
6	12	3	3	22	56	6
4	54	97	2	21	15	3
4	22	31	2	36	24	3
4	11	81	2	27	29	5
4	43	88	2	50	45	4
5	36	72	3	13	68	4
3	6	37	2	39	82	1
4	50	16	2	34	91	4
3	40	6	2	32	75	3
4	53	78	2	53	90	5
6	1	50	3	20	85	5

Midday Peak 1-mile Raw Data

Total Time			Running Time			Number of Stops
min	sec	ms	min	sec	ms	
9	12	41	3	34	11	5
3	0	52	2	40	52	2
4	30	72	2	58	51	3
7	6	97	3	46	83	4
3	7	65	2	20	8	4
4	5	15	2	27	96	3
3	37	53	2	29	12	5
5	41	97	3	25	1	5
12	26	25	3	29	76	4
3	19	50	2	10	0	2
9	53	32	4	24	64	9
5	19	81	3	6	89	5
3	56	91	2	53	63	4
4	16	88	2	59	44	3
6	34	81	3	45	59	5
9	27	19	4	4	97	11
5	3	93	3	11	9	4
4	18	44	2	25	40	3
3	34	66	2	16	47	2
5	22	78	3	0	28	4
3	52	62	2	45	84	2
3	10	41	2	8	44	2
4	14	44	2	22	4	2
3	50	6	2	16	56	2
3	27	78	2	27	51	2
4	7	21	2	38	56	2
4	24	97	2	40	90	4
7	20	63	3	59	73	9
4	54	88	3	13	44	3
8	8	34	4	15	23	10
3	2	53	2	35	93	2
3	34	5	2	44	84	2
3	26	50	2	43	7	2
5	46	34	3	23	25	5
7	15	15	3	26	66	8
6	20	50	3	14	94	5
4	20	94	3	18	6	4
3	56	78	3	13	76	3
4	14	69	2	55	8	2
3	46	59	2	38	53	4
3	34	65	2	24	19	2
9	36	94	4	17	13	10

PM Peak 1-mile Raw Data

Total Time			Running Time			Number of Stops
min	sec	ms	min	sec	ms	
8	58	9	4	3	62	10
5	12	34	3	20	99	4
7	24	97	4	2	27	5
6	38	56	4	6	85	8
4	36	12	2	58	60	2
9	18	91	4	13	43	9
4	56	0	3	21	20	4
5	2	22	2	35	26	4
3	51	85	2	43	99	5
5	42	0	2	38	17	4
4	43	38	2	32	74	5
5	39	88	2	46	27	5
2	22	78	2	6	33	1
4	36	3	2	24	74	2
3	7	65	2	14	9	2
3	43	60	2	39	67	3
5	5	60	3	21	55	5
5	37	19	3	19	57	4
3	14	0	2	18	83	3
9	21	41	4	7	61	7
3	9	3	2	14	47	1
4	37	40	2	28	21	4
8	32	75	3	38	76	7
3	32	38	2	22	78	4
4	3	34	3	40	73	2
6	0	15	3	1	7	4
9	44	47	3	3	86	7
2	15	63	2	5	47	2
4	8	59	2	22	55	4
3	19	62	2	26	79	2
6	47	94	3	4	97	6
4	55	71	2	51	82	5
4	55	31	3	47	51	5

AM Peak 2-min Raw Data

Distance (mi)		Run Time			Number of Stops
Starting	Ending	min	sec	ms	
114.5	115.2	1	36	40	1
115.3	115.7	1	10	91	2
115.7	116.2	1	11	50	2
116.3	116.8	1	17	10	3
117	117.2	1	22	31	1
117.5	117.8		52	97	1
117.8	118.6	1	46	73	3
118.7	118.8	1	12	15	2
118.8	119.1	1	14	3	3
119.1	119.2	1	2	17	4
119.4	119.9	1	12	71	1
120.1	120.5		51	74	1
120.8	121		40	50	2
121.1	121.3		42	65	2
121.3	121.7	1	9	19	1
121.8	122	1	8	91	2
122	122.2		39	20	3
122.3	123	1	38	38	1
123.2	123.7	1	28	56	1
123.7	124.1	1	7	64	1
124.3	124.9	1	38	36	2
125	125.9	1	48	81	1
126	126.3	1	15	52	4
126.3	126.9	1	46	15	1
127.1	127.8	1	57	33	1
128	128.3		54	22	2
128.4	128.7	1	5	34	3
128.8	129.1	1	2	79	2
129.3	129.8	1	22	22	2
129.8	130.1	1	29	34	1
130.1	130.7	1	47	34	1
130.7	131.1	1	21	77	3
131.1	131.4	1	8	69	2
0.1	0.7	1	36	37	2
0.8	1.3	1	20	13	3
1.8	2.2	1	24	94	1
2.3	2.5	0	36	56	2
2.6	3.1	1	36	4	3
3.5	3.9	0	57	31	2
3.9	4.1	0	42	25	3
4.1	4.5	1	7	10	2
4.6	5.3	1	46	49	1
5.3	6.1	1	26	85	2
6.1	6.4	0	36	84	1
6.5	7	1	14	75	2

7.2	8.3	2	0	0	0
8.6	9	0	56	60	1
9.2	9.5	0	57	21	3
9.6	10.6	1	49	34	2
10.7	11.4	1	34	43	3
11.4	11.5	1	10	12	3
11.5	12.1	1	30	60	1
12.1	12.6	1	4	84	1
12.6	13.3	1	27	69	2
13.3	14.2	1	50	40	1
14.3	14.4	0	35	3	3
14.5	15.2	1	50	66	1
15.5	15.6	0	59	53	2
15.6	16.1	1	32	73	1
16.2	16.7	1	3	63	1
16.7	16.8	0	20	47	2
16.8	17.5	1	42	6	2
17.6	17.8	0	38	9	1
192.1	192.8	1	54	50	1
193	193.5	1	25	63	2
193.7	193.9		57	99	3
194	194.3	1	11	40	2
194.4	195.1	1	29	59	2
195.2	195.6	1	9	25	3
195.7	196.1		57	6	2
196.3	196.8	1	7	75	1
196.9	197.2	1	13	41	3
197.3	197.9	1	36	72	2
198.1	198.4		39	72	2
198.5	199	1	27	82	3
199.1	199.3		43	69	1
199.4	199.8	1	25	19	2
199.8	199.9		40	28	3
200	200.1		51	43	3
200.1	200.3	1	27	75	3
200.4	200.6		54	34	1
200.7	200.9	1	5	5	1
201.4	201.8	1	5	40	2
201.9	201.95		26	44	2
202	202.7	2	0	0	0
202.8	203.1	1	14	59	2
203.2	203.5	1	23	15	3
203.8	204.2	1	30	39	3

Midday Peak 2-min Raw Data

Distance (mi)		Run Time			Number of Stops
Starting	Ending	min	sec	ms	
58.4	58.6	0	53	15	2
58.6	59.1	1	50	59	2
59.1	59.6	1	40	40	1
59.7	60.6	1	11	41	1
60.1	60.8	1	11	27	1
60.9	61.3	0	58	32	2
61.5	62	1	21	48	2
62.1	62.6	1	36	11	3
62.6	62.8	0	38	29	3
62.8	63.7	1	45	75	1
64.4	65.4	1	33	58	2
65.4	65.6	1	9	13	2
65.7	66.3	1	20	75	1
66.4	67	1	18	4	1
67.1	67.6	1	28	60	2
67.8	68.3	1	19	75	2
68.3	68.8	1	18	72	2
68.9	69.2	0	57	7	3
69.2	69.7	1	20	84	2
69.8	70.2	1	11	77	1
70.3	71	1	32	93	3
71.6	71.9	1	6	22	2
72	72.6	1	36	22	1
72.7	72.9	0	36	71	2
73	73.7	1	15	97	1
73.8	74.2	1	56	68	1
74.5	74.9	1	19	7	2
75	75.4	1	36	34	2
75.4	76	1	32	12	1
76	76.7	1	34	40	3
76.8	77.3	1	15	96	1
77.4	77.9	1	18	9	1
77.9	78.4	1	30	29	3
78.5	79	1	29	31	1
140.6	141.2	1	34	34	2
141.4	142	1	24	29	2
142.2	142.6	1	31	57	1
142.8	143.6	1	56	45	1
143.8	144.1		49	85	1
144.3	144.8	1	15	49	2
145.7	146.1	1	36	9	2
146.1	146.9	1	42	28	2
147.2	147.7	1	11	18	2
147.8	148.4	1	20	88	2
148.5	149		56	97	1

149.1	149.7	1	48	56	2
150	150.6	1	42	44	1
150.6	150.9	1	0	83	2
151.3	152	2	0	0	0
152	152.6	1	32	40	2
152.8	153.4	1	53	30	2
153.7	153.8	0	40	47	2
154	154.1	0	40	29	1
154.2	154.6	1	13	87	3
154.7	154.8		40	0	1
154.9	155.7	1	56	93	1
156	156.2		47	38	1
156.3	156.7		53	41	1
156.8	157.3	1	43	87	2

PM Peak 2-min Raw Data

Distance (mi)		Run Time			Number of Stops
Starting	Ending	min	sec	ms	
169.1	169.4	1	10	24	2
169.4	169.9	1	28	31	1
170.1	170.7	1	30	41	2
171.3	171.6		53	81	1
171.8	172		52	94	3
172	172.1		41	16	4
172.1	172.2		32	84	4
172.2	172.3		33	43	4
172.3	172.4		33	57	3
172.5	173.4	1	58	70	1
173.7	174.1	1	8	97	2
174.2	174.4		55	91	2
174.4	175	1	20	70	1
175.3	175.7		54	93	2
175.7	175.9	1	0	14	6
176.2	176.5	1	11	11	2
176.7	177	1	3	34	3
177.2	177.6	1	17	84	2
177.8	178.5	1	47	76	1
178.5	178.8	1	8	13	3
179	179.3		55	17	2
179.5	179.8		49	28	2
180	180.4	1	27	91	2
180.5	180.6		48	91	2
180.7	180.9		48	51	4
181	181.3		53	10	3
181.3	181.6		55	44	2
181.7	182.3	1	50	31	1
182.3	182.6	1	2	94	3
118.5	119.2	1	51	41	1
119.2	119.6	1	19	84	3
119.6	120	1	5	90	2
120.7	121.1	0	56	50	2
121.1	121.3	1	5	22	3
121.3	121.7	1	15	6	2
121.7	122	0	54	62	2
122.2	122.6	1	12	13	2
122.6	122.8	0	34	37	1
122.9	123.2	1	7	50	2
123.2	123.6	0	59	53	2
123.6	124	1	17	33	2
124.1	124.3	1	0	37	3
124.3	124.4	0	41	91	2
124.4	125.3	1	51	0	1
125.4	126	1	16	75	1

126.3	127	1	30	66	1
127	127.7	1	38	35	2
127.8	127.9	0	48	28	2
127.9	128.3	1	26	46	4
128.4	129	1	16	22	2
129.1	129.6	1	3	51	2
129.6	130.1	0	50	0	2
130.7	131.5	1	44	75	1
131.5	131.8	0	49	10	1
131.9	132.8	2	0	0	0
132.8	133.1	1	26	60	3
133.1	133.6	1	13	72	1
133.7	134.3	1	26	18	2
134.4	135.1	1	29	52	1
135.1	135.3	0	48	47	3

APPENDIX B: NOVEMBER 2008 RAW DATA

AM Peak 1-mile Raw Data

Total Time			Stopped Time			Number of Stops
min	sec	ms	min	sec	ms	
4	12	0	1	42	0	4
3	33	0	1	8	0	2
2	34	0	0	20	0	2
4	40	0	1	57	0	4
5	13	0	2	20	0	5
3	42	0	0	50	0	1
6	42	0	3	9	0	6
7	57	0	5	12	0	3
3	21	0	1	22	0	3
4	17	0	1	29	0	5
6	15	0	2	41	0	6
5	26	0	3	31	0	5
3	8	0	0	49	0	2
2	30	0	0	0	0	1
3	49	0	0	50	0	1
3	25	0	0	11	0	3
4	36	0	0	49	0	3
3	32	10	1	12	13	4
1	56	84	0	35	0	1
2	52	10	0	40	19	1
4	6	43	1	46	25	3
3	54	75	1	16	57	2
4	35	72	1	39	37	1
4	56	41	1	58	65	2
3	57	16	1	8	39	2
4	2	75	1	23	54	2
3	36	9	0	34	34	2
5	37	28	2	21	69	4
3	12	41	0	54	9	3
6	18	56	3	32	74	3
4	54	68	1	25	45	3
7	7	75	3	40	29	4
4	17	44	1	28	75	3
6	6	59	3	8	18	5
2	51	21	0	28	3	1
2	34	52	0	18	22	1
4	9	82	1	36	37	4
4	24	16	1	40	10	4
3	28	14	1	10	70	4
3	53	38	1	29	84	2
4	40	34	2	29	11	3
4	31	54	1	24	89	3
5	29	87	2	1	9	3
4	2	40	1	35	41	3

3	28	46	1	6	45	4
2	18	20	0	22	65	1
3	29	47	1	33	70	2
5	32	98	2	21	40	4
4	10	19	0	37	9	3
3	31	92	1	12	16	5
3	36	44	0	41	8	4
4	23	81	2	4	44	2
5	28	47	2	51	35	3
3	39	59	1	10	5	2
3	46	64	0	37	19	1
2	47	60	0	18	78	1
6	43	34	3	36	9	5
5	26	81	2	44	46	4
4	47	37	2	10	27	3
4	12	60	0	59	31	2
3	0	31	0	26	41	1
4	14	53	1	21	16	3
4	12	44	1	39	97	3
3	16	7	0	39	83	2
4	31	90	1	14	19	2

Midday Peak 1-mile Raw Data

Total Time			Stopped Time			Number of Stops
min	sec	ms	min	sec	ms	
5	28	0	1	34	0	5
2	18	0	0	2	0	1
3	44	0	1	3	0	3
4	55	0	2	7	0	3
4	34	0	1	32	0	2
3	7	0	0	41	0	3
4	14	0	1	43	0	3
3	2	0	1	30	0	2
2	38	0	0	17	0	3
2	41	0	0	23	0	1
4	3	0	0	42	0	3
4	45	0	2	21	0	4
1	56	0	0	0	0	0
3	17	0	0	56	0	1
3	3	0	0	36	0	3
4	27	0	1	59	0	7
3	39	0	1	9	0	4
3	5	69	0	38	1	1
4	8	94	1	32	59	2
4	53	47	2	5	89	3
3	9	62	0	14	19	1
4	5	66	1	20	73	3
5	53	22	2	47	5	4
4	25	59	1	3	12	2
4	26	34	1	37	76	3
4	28	10	1	34	5	2
4	35	71	1	46	3	3
3	11	30	0	27	92	1
3	8	90	0	42	75	1
4	33	34	1	55	28	2
3	37	56	0	45	9	2
6	10	12	2	5	73	4
4	36	85	1	43	40	4
4	23	75	0	51	34	
4	35	69	1	21	58	3
5	59	41	1	59	4	8
4	53	97	2	29	23	4
3	36	9	1	4	90	3
5	0	80	2	21	20	2
5	38	0	2	10	0	3
5	33	20	2	48	69	3
4	18	34	1	32	0	3
2	17	78	0	5	60	1
3	29	50	0	40	10	2
2	49	62	0	22	26	3

4	8	81	1	53	88	2
3	58	84	1	26	10	3
4	51	20	1	20	43	3
4	7	64	1	23	62	3
6	0	70	2	52	91	3
7	3	21	3	42	39	6
4	22	0	1	24	0	4
5	25	0	2	13	0	7
3	3	0	0	45	0	3
5	11	0	2	22	0	6
3	4	0	0	54	0	4
3	13	0	0	42	0	1
4	23	0	1	56	0	2
4	9	0	1	15	0	2
2	17	0	0	13	0	1
2	45	0	0	39	0	2
5	34	0	2	12	0	3
5	51	0	3	19	0	3
4	54	0	2	28	0	3

PM Peak 1-mile Raw Data

Total Time			Stopped Time			Number of Stops
min	sec	ms	min	sec	ms	
6	52	52	3	9	63	5
4	3	46	1	8	15	2
5	28	57	2	31	11	5
5	56	85	2	9	31	6
3	39	59	1	1	27	2
3	34	65	0	53	84	4
3	41	72	1	22	35	2
3	52	95	0	49	99	3
5	32	51	2	20	6	4
3	39	55	1	45	0	2
5	38	5	2	43	29	4
5	20	91	2	19	25	4
4	40	4	1	49	53	4
4	20	14	2	2	74	5
4	29	0	1	22	96	3
4	3	53	1	8	56	3
8	52	52	4	1	29	9
2	15	47	0	3	78	1
4	49	96	1	40	55	2
4	19	19	1	33	96	3
8	16	47	4	35	16	7
4	30	59	1	26	45	4
4	30	57	1	18	56	3
6	3	42	2	55	57	4
7	12	91	3	52	74	8
5	29	29	2	15	55	5
5	57	35	1	59	1	7
2	54	17	0	4	2	2
12	53	85	8	42	97	11
5	35	55	2	20	65	4
4	5	40	1	22	25	3
4	36	84	2	22	27	5
4	55	31	1	49	50	4
7	3	88	4	23	67	4
2	59	64	0	59	13	2
16	42	13	10	46	88	16
3	47	87	0	49	89	2
4	57	19	1	54	85	3
4	29	59	1	44	8	3
4	17	78	1	54	0	4
25	54	87	17	55	52	
6	35	97	3	16	10	4
4	32	19	1	36	84	4
3	38	13	0	36	53	2
6	2	0	2	15	17	

AM Peak 2-min Raw Data

Distance (mi)		Stopped Time			Number of Stops
Starting	Ending	min	sec	ms	
73.9	74.2	1	14	37	1
74.2	74.4	1	19	59	3
74.4	74.9	1	6	3	2
75	75.6	0	3	37	1
75.6	75.9	1	10	13	2
76	76.7	1	12	12	1
76.8	77	1	29	0	2
77.8	78.4	0	36	56	2
78.4	79.2	0	21	4	1
79.3	79.6	0	50	84	2
79.6	80.4	0	22	46	2
80.5	81.3	0	26	85	1
81.4	82.1	0	36	90	2
82.1	82.7	0	34	10	3
82.7	82.8	1	25	28	3
82.8	83.4	0	22	22	2
83.4	84.1	0	42	25	1
84.2	84.6	0	59	17	2
84.6	84.7	1	27	37	2
84.7	85	1	17	10	2
85	85.5	0	32	75	3
85.6	85.9	1	14	63	2
86	86.4	1	0	46	1
86.4	86.8	1	4	10	2
86.9	87.2	0	59	5	2
87.2	88.1	0	7	81	1
88.1	88.7	0	40	28	2
89.8	90.3	0	45	79	1
90.3	91.1	0	7	69	1
91.1	91.9	0	30	19	1
92	92.4	0	17	75	2
10	10.3	1	10	78	2
10.5	11	0	22	54	3
11.2	11.7	0	36	21	2
11.8	12.5	0	16	97	1
12.7	12.9	1	19	12	2
13	13.4	0	41	63	1
13.5	14	0	54	72	1
14.2	14.5	1	10	88	2
14.6	14.8	1	10	75	2
14.9	15.3	0	51	37	1
15.3	16.1	0	0	0	0
16.2	16.6	0	30	24	1
16.7	17	0	54	6	1

17.1	17.4	1	5	69	2
17.5	18	0	50	63	1
18.1	18.4	0	49	77	2
18.5	18.6	1	24	32	3
18.7	19.2	0	16	37	2
19.3	19.9	0	29	22	2
20	20.5	0	18	50	2
20.7	21	1	7	47	3
21.1	21.3	1	6	0	3
21.4	21.8	0	30	10	1
21.9	22.3	0	34	19	1
22.4	22.9	0	26	78	1
23	23.6	0	19	33	1
23.7	24.2	0	33	69	2
24.3	24.5	1	2	47	3

Midday Peak 2-min Raw Data

Distance (mi)		Stopped Time			Number of Stops
Starting	Ending	min	sec	ms	
16.5	17.1	0	37	0	2
17.2	17.9	0	23	87	1
18.1	18.5	1	0	12	2
18.5	19.1	0	34	88	2
19.1	19.6	0	41	65	2
19.6	20.1	0	37	51	3
20.1	20.7	0	30	68	2
20.8	21.3	0	44	28	2
21.3	21.4	0	49	56	4
21.4	21.8	0	43	4	1
21.8	22.2	1	0	26	1
22.2	22.6	0	17	68	3
22.6	23.2	0	4	78	1
23.2	24.1	0	2	22	1
24.2	24.5	0	42	4	3
25.3	26.1	0	11	14	2
26.2	26.7	0	34	61	3
26.7	27.5	0	17	94	2
27.6	28.1	0	45	8	3
28.1	28.5	0	32	93	1
28.9	29.2	0	11	82	1
29.3	29.9	0	25	9	1
30	30.5	0	40	94	1
30.5	31.2	0	24	59	1
31.3	31.6	0	50	22	2
34.6	34.7	1	33	78	1
34.7	35.3	0	47	72	2
35.3	36	0	10	72	1
36.1	36.6	0	6	72	2
35	35.7	0	10	79	1
35.9	36.4	0	42	79	1
36.5	37.2	0	14	87	1
37.3	37.6	0	56	75	1
37.7	37.9	1	29	16	2
38	38.6	0	20	84	1
38.7	38.9	0	37	40	1
39	39.3	0	56	53	2
39.4	40.1	0	18	62	1
40.2	40.7	0	30	87	1
40.8	41.4	0	15	75	1
42	42.2	1	9	44	2
42.3	42.7	0	26	41	1
42.8	43.4	0	17	72	2
43.5	43.8	0	45	19	1
43.9	44.1	0	49.69	2	

44.2	44.7	0	2	94	1
44.8	45.5	0	4	40	1
45.6	45.9	0	58	65	2
46	46.6	0	12	99	1
47.4	48	0	1	88	1
48.2	48.6	0	41	32	2
48.7	49.2	0	13	59	1
49.3	49.9	0	9	50	1
50	50.8	0	4	18	1
50.9	51.6	0	14	35	1
51.7	51.9	1	4	16	3
52	52.2	0	49	47	2

PM Peak 2-min Raw Data

Distance (mi)		Stopped Time			Number of Stops
Starting	Ending	min	sec	ms	
73.8	74.3	0	28	18	3
74.3	74.5	1	16	47	2
74.6	75.1	0	56	50	1
75.3	75.6	0	36	22	2
75.6	75.8	1	18	34	1
75.8	76.3	0	57	56	2
76.4	76.8	0	39	37	1
76.9	77.5	0	24	93	3
77.5	77.7	1	6	22	1
77.7	77.9	1	14	78	2
78	78.5	0	24	47	1
78.6	79.3	0	16	5	2
79.4	80.1	0	5	16	1
80.2	80.6	0	17	22	2
80.6	80.8	1	10	14	1
80.9	81.2	1	2	31	1
81.2	81.4	1	11	93	1
81.4	82.2	0	8	34	1
82.3	82.6	1	17	13	1
82.7	83.3	0	46	72	2
83.4	84	0	19	79	3
84	84.4	0	39	71	3
84.4	84.7	0	55	19	2
84.8	85.5	0	15	46	1
85.6	86.1	0	38	79	1
86.1	86.6	0	40	84	1
86.7	87.2	0	55	81	3
87.2	87.7	0	40	81	2
87.7	88	1	4	78	2
88.1	88.5	0	59	18	2
88.6	89	0	48	38	2
89	89.4	1	0	37	2
89.5	89.9	0	47	28	2
90	90.5	0	32	0	1
90.5	91.3	0	3	28	1
91.3	91.9	0	31	59	2
64.6	65	0	37	7	2
65.1	65.4	0	52	22	3
65.5	65.6	1	31	94	3
65.7	66.2	0	41	82	2
66.3	66.8	0	30	56	3
66.9	67.3	0	24	26	2
67.4	67.7	0	41	2	1
67.8	68.1	0	46	41	2
68.2	68.8	0	15	0	1

69	69.4	0	56	4	2
69.5	70.1	0	42	85	1
70.2	70.7	0	16	4	1
70.8	71.3	0	49	28	1
71.4	71.6	1	17	3	2
71.7	72.1	0	36	73	1
72.2	72.5	1	0	29	2
72.6	72.9	0	48	46	2
73	73.4	0	15	22	1
73.5	73.7	1	5	18	3
73.8	74.3	0	22	16	2
74.4	74.8	0	42	25	1
74.9	75.5	0	13	7	1
75.6	76.1	0	42	78	1
76.2	76.8	0	21	34	1
76.9	77.3	0	54	44	2
77.4	77.6	1	19	44	2
77.7	78.2	0	37	16	1
78.3	78.7	0	15	58	1

LIST OF REFERENCES

[1] Prigogine, I. and R. Herman (1971). "Kinetic Theory of Vehicular Traffic", American Elsevier

[2] Mahmassani H., J. C. Williams and R. Herman (1984). "Investigation of Network-Level Traffic Flow Relationships: Some Simulation Results", Transportation Research Record 971, Transportation Research Board, pp. 121-130.

[3] Williams, J. C., H. S. Mahmassani, and R. Herman (1985). "Analysis of Traffic Network Flow Relations and Two-Fluid Model Parameter Sensitivity", Transportation Research Record 1005, Transportation Research Board

[4] Ardekani, S. A. (1984). "The Two-Fluid characterization of Urban Traffic: Theory Observation, and Experiment", Ph.D. Dissertation, University of Texas at Austin

[5] Mattingly, S. P., P. T. Vo, S. A. Ardekani and Y. Dilshad (2007). "Comparison of the Quality of Service in the Arlington, Dallas, Fort Worth CBD – A Two Fluid Model Approach." Transportation Research Board, 86th Annual Meeting, paper# 07-0804

[6] Ayadh, M. T. (1986). "Influence of the City Geometric Features on the Two Fluid Model Parameters", M.S. Thesis, Virginia Polytechnic Institute and State University

[7] Ardekani, S. A., J. C. Williams and S. Bhat (1992) " Influence of Urban Network Features on Quality of Traffic Service" Transportation Research Record 1358, pp. 6-12

[8] Bhat, S .C. S. (1994). "Effects of Geometric and Control Features on Network Traffic: A Simulation Study." Ph.D. Dissertation, University of Texas at Arlington

[9] Dowling, R., A. Skabardonis, J. Halkais, G. McHale and G. Zammit (2004). "Guidelines for Calibration of Microsimulation Models", Transportation Research Record 1876, Transportation Research Board, pp. 1-9.

[10] Jha, M., G. Gopalan, A. Garms, B. P. Mahanti, T. Toledo and M. E. Ben-Akiva (2004). "Development and Calibration of a Large-Scale Microscopic Traffic Simulation Model", Transportation Research Record 1876, Transportation Research Board, pp. 121-131.

[11] Toledo, T., M. E. Ben-Akiva, D. Darda, M. Jha and H. N. Koutsopoulos (2004). "Calibration of Microscopic Traffic Simulation Models with Aggregate Data", Transportation Research Record 1876, Transportation Research Board, pp. 10-19.

[12] Herman, R., L. A. Malakhoff and S. A. Ardekani (1988). "Trip Time-Stop Time Studies of Extreme Driver Behaviors", Transportation Research Part A, Vol. 22A, No. 6, pp.427-433.

[13] PTV, Traffic Mobility Logistics, (2007). VISSIM 4.30 Users Manual. Karlsruhe, Germany: Planung Transport Verkehr.